20. Shen, L. P., Pictet, R. L., and Rutter, W. J. (1982) Human somatostatin I: sequence of the cDNA. *Proc. Natl. Acad. Sci. U. S. A.* **79,** 4575–4579
21. Minamino, N., Kangawa, K., and Matsuo, H. (1984) Neuromedin C: a bombesin-like peptide identified in porcine spinal cord. *Biochem. Biophys. Res. Commun.* **119,** 14–20
22. Brosch, M., Swamy, S., Hubbard, T., and Choudhary, J. (2008) Comparison of Mascot and XITandem performance for low and high accuracy mass spectrometry and the development of an adjusted mascot threshold. *Mol. Cell. Proteomics* **7,** 962–970
23. Fälth, M., Sköld, K., Norrman, M., Svensson, M., Fenyö, D., and Andren, P. E. (2006) SwePep, a database designed for endogenous peptides and mass spectrometry. *Mol. Cell. Proteomics* **5,** 998–1005
24. Kieffer, A. E., Goumon, Y., Ruh, O., Chasserot-Golaz, S., Nullans, G., Gasnier, C., Aunis, D., and Metz-Boutigue, M. H. (2003) The N- and C-terminal fragments of ubiquitin are important for the antimicrobial activities. *FASEB J.* **17,** 776–778
25. Bock-Marquette, I., Saxena, A., White, M. D., Dimaio, J. M., and Srivastava, D. (2004) Thymosin beta4 activates integrin-linked kinase and promotes cardiac cell migration, survival and cardiac repair. *Nature* **432,** 466–472
26. Pan, H., Che, F. Y., Peng, B., Steiner, D. F., Pintar, J. E., and Fricker, L. D. (2006) The role of prohormone convertase-2 in hypothalamic neuropeptide processing: a quantitative neuropeptidomic study. *J. Neurochem.* **98,** 1763–1777
27. Orr, D. F., Chen, T., Johnsen, A. H., Chalk, R., Buchanan, K. D., Sloan, J. M., Rao, P., and Shaw, C. (2002) The spectrum of endogenous human chromogranin A-derived peptides identified using a modified proteomic strategy. *Proteomics* **2,** 1586–1600

GLIA 57:1082–1090 (2009)

The Alzheimer's Disease Drug Memantine Increases the Number of Radial Glia-like Progenitor Cells in Adult Hippocampus

TAKASHI NAMBA,[1] MOTOKO MAEKAWA,[2] SHIGEKI YUASA,[2] SHINICHI KOHSAKA,[1]* AND SHIGEO UCHINO[1]
[1]*Department of Neurochemistry, National Institute of Neuroscience, Kodaira, Tokyo, Japan*
[2]*Department of Ultrastructural Research, National Institute of Neuroscience, Kodaira, Tokyo, Japan*

KEY WORDS
neurogenesis; NMDA receptor; GFAP; proliferation; nestin; Sox2

ABSTRACT
New neurons are continuously generated in the hippocampus of the adult mammalian brain, and *N*-methyl-D-aspartate receptor (NMDA-R) antagonists have been found to increase the number of newly generated neurons in the dentate gyrus (DG) of the adult hippocampus. In this study, we examined the effect of memantine, an NMDA-R antagonist that is clinically used for the treatment of Alzheimer's disease, on primary progenitor cells exhibiting a radial glia-like (RGL) morphology in the DG. We injected 3-month-old mice with memantine (50 mg/kg body weight, intraperitoneally [i.p.]); 3 days later, we injected the mice with 5-bromo-2-deoxyuridine (BrdU; 75 mg/kg body weight, i.p.). We then counted the number of BrdU-labeled RGL progenitor cells in the DG 1 or 7 days after the BrdU-injection. The number of BrdU-labeled RGL progenitor cells had increased significantly by 5.1-fold on day 1 and by 13.7-fold on day 7 after BrdU-injection. Immunohistochemical staining revealed that the BrdU-labeled RGL progenitor cells expressed two primary progenitor cell marker proteins, nestin and Sox2. These results clearly demonstrated that memantine promotes the proliferation of RGL progenitor cells. We also found that memantine increased the ratio of horizontally aligned RGL progenitor cells, which are probably produced by symmetric division. These findings suggest that memantine increases the proliferation of primary progenitor cells and expands the primary progenitor cell pool in the adult hippocampus by stimulating symmetric division.

INTRODUCTION

The generation of new neurons, so-called neurogenesis, persists throughout life in the hippocampus of mammals, including humans (Altman and Das, 1965; Eriksson et al., 1998; Kuhn et al., 1996; Maekawa et al., 2005; Namba et al., 2005; Seki and Arai, 1993, 1995). Neural progenitor cells divide and give rise to new neurons in at least two regions of the adult brain: the dentate gyrus (DG) of the hippocampus and the subventricular zone of the lateral ventricle (Doetsch et al., 1999; Fukuda et al., 2003; Seki et al., 2007; Seri et al., 2001). Neurogenesis in the hippocampus associated with synaptic plasticity (Schmidt-Hieber et al., 2004) and cognitive functions, including learning and memory (Becker and Wojtowicz, 2007; Kee et al., 2007; Wojtowicz et al., 2008). The initial step in hippocampal neurogenesis is the proliferation of progenitor cells in the subgranular zone (SGZ) of the DG, which contains several types of progenitor cells (Filippov et al., 2003; Fukuda et al., 2003; Seki et al., 2007; Seri et al., 2004; von Bohlen Und Halbach, 2007). Primary progenitor cells, which are characterized by the expression of glial fibrillary acidic protein (GFAP) and nestin, extend their radial processes across the granule cell layer (GCL), exhibit a radial glia-like (RGL) morphology, and then divide to produce intermediate progenitor cells. The intermediate progenitor cells generate immature neurons, which migrate into the GCL where they differentiate into mature granule neurons and ultimately contribute to the local neural network (van Praag et al., 2002).

Neurogenesis in the DG is promoted not only by pathological factors, such as ischemia, epileptic seizures, and traumatic brain injury (Liu et al., 1998; Parent et al., 1997), but also by various physiological factors, including growth factors, neurotransmitters, an enriched environment, learning and exercise (reviewed in Abrous et al., 2005). Glutamate signaling is also involved in hippocampal neurogenesis. Our recent study and a study by Jin et al. (2006) showed that memantine, an uncompetitive *N*-methyl-D-aspartate receptor (NMDA-R) antagonist that is clinically used for the treatment of Alzheimer's disease, increases the cell proliferation and promotes the subsequent production of mature neurons, similar to other NMDA-R antagonists, such as MK-801, D(−)-2-amino-5-phosphonopentanoic acid (D-APV), and CGP-43487 (Cameron et al., 1995; Hirasawa et al., 2003; Nacher et al., 2001). However, because the mechanism

Additional Supporting Information may be found in the online version of this article.

Grant sponsors: Ministry of Health, Labour and Welfare of Japan, The Program for the Promotion of Fundamental Studies in Health Science of the National Institute of Biomedical Innovation.

Motoko Maekawa is currently at Laboratory for Molecular Psychiatry, RIKEN Brain Science Institute, 2-1 Hirosawa, Wako, Saitama 351-0198, Japan.

*Correspondence to: Shinichi Kohsaka, Department of Neurochemistry, National Institute of Neuroscience, 4-1-1 Ogawahigashi, Kodaira, Tokyo 187-8502, Japan. E-mail: kohsaka@ncnp.go.jp

Received 24 June 2008; Accepted 10 November 2008

DOI 10.1002/glia.20831

Published online 29 December 2008 in Wiley InterScience (www.interscience.wiley.com).

TABLE 1. Antibodies

Marker	Species, isotype	Label	Working dilution	Vendor
Primary antibodies				
BrdU	Rat IgG	None	1:400	ImmunologicalsDirect.com, UK
GFAP	Mouse IgG	None	1:2000	Sigma, Mo, USA
GFAP	Rabbit IgG	None	1:800	Dako, Denmark
Nestin	Mouse IgG	None	1:400	BD Bioscience, CA, USA
PSA-NCAM	Mouse IgM	None	1:800	Seki and Arai (1991)
Sox2	Rabbit IgG	None	1:2000	Chemicon International, CA, USA
Secondary antibodies				
Anti-mouse IgG	Donkey IgG	Cy5	1:200	Jackson, PA, USA
Anti-mouse IgM	Donkey IgG	Cy5	1:200	Jackson
Anti-rabbit IgG	Donkey IgG	Cy2	1:200	Jackson
Anti-rabbit IgG	Donkey IgG	Cy5	1:200	Jackson
Anti-rat IgG	Donkey IgG	Cy3	1:200	Jackson

responsible for the stimulation of cell proliferation by NMDA-R antagonists remains unknown, in the present study we focused on primary progenitor cells exhibiting a RGL morphology and examined the effect of memantine on their proliferation. The present results clearly demonstrated that memantine promotes the proliferation of RGL progenitor cells and the subsequent expansion of the RGL progenitor cell pool in the GCL by stimulating symmetric division.

MATERIALS AND METHODS

Three-month-old male C57BL6/J mice (Clea Japan, Tokyo, Japan) were used in this study. All experimental procedures were approved by The Animal Care and Use Committee of the National Institute of Neuroscience.

Animals and Drug Administration

Mice were injected with memantine (Sigma, St. Louis, MO) at a dose of 50 mg/kg body weight i.p. or with the same volume of 0.9% saline (Ohtsuka Pharmaceuticals, Tokyo, Japan), as a control. The dose of memantine was determined as that sufficient to promote the proliferation of RGL progenitor cells in pilot studies. Three days later, the mice were injected with BrdU (Sigma) at a dose of 75 mg/kg body weight i.p. on three separate occasions at an interval of 2 h. The mice were then sacrificed on day 1, 2 or day 7 after the BrdU-injection.

Tissue Preparation

Mice were deeply anesthetized with sodium pentobarbital (Kyoritsu Pharmaceuticals, Tokyo, Japan) and then transcardially perfused with 4% paraformaldehyde in 0.1-M phosphate buffer. Their brains were removed and immersion-fixed for 24 h at 4°C in the same fixative. After washing in phosphate-buffered saline (PBS), the brains were successively equilibrated in 10% and 20% sucrose in PBS. The cerebral cortices containing the hippocampal formation were dissected away from the remaining brain structure. Next, 1- to 2-mm-thick slices were cut from the medial part of the hippocampus in a plane perpendicular to the septo-temporal axis of the hippocampal formation, embedded in Tissue-Tek optimal cutting temperature compound (Sakura, Tokyo, Japan), and frozen with liquid nitrogen (Seki et al., 2007).

Immunohistochemistry

Immunohistochemistry was performed using a floating method, as described previously (Namba et al., 2005, 2007). Frozen brains were sliced into 40-μm sections with a cryostat (CM-3000; Leica, Nussloch, Germany). After washing the sections with PBS, they were incubated at 4°C for 72 h in PBS containing 1% bovine serum albumin (BSA), 1% normal donkey serum, and 0.1% triton X-100 plus one of the primary antibodies shown in Table 1. To stain poly-sialylated neural cell adhesion molecule (PSA-NCAM), the sections were pretreated with 100% methanol (Seki and Arai, 1991). After washing in PBS, the sections were then incubated at room temperature for 1–2 h in PBS containing 1% BSA plus an appropriate secondary antibody shown in Table 1. For immunostaining with anti-BrdU antibody, the sections were incubated in 2 N HCl at 37°C for 35 min after staining with the other antibodies (anti-GFAP and anti-Nestin antibodies or anti-GFAP and anti-Sox2 antibodies and the appropriate secondary antibodies), neutralized with 0.1-M borate buffer (pH 8.5), and then incubated with anti-BrdU antibody (Table 1) at 4°C for 24 h in PBS containing 1% BSA. After washing in PBS, the sections were incubated at room temperature for 1–2 h in PBS containing 1% BSA plus Cy3-conjugated anti-rat IgG antibody (Table 1). The sections were mounted on a glass slide (SUPERFROST; Matsunami, Osaka, Japan), and examined for fluorescent signals using a confocal laser-scanning microscope (CLSM) with 20×, 40×, and 60× objectives (FV1000; Olympus, Tokyo, Japan).

Cell Counting

To measure the number of GFAP- or Nestin-positive RGL progenitor cells or PSA-NCAM-positive cells in the GCL including the SGZ, an average of five sections per mouse was analyzed (see Fig. 1). We defined RGL progenitor cells as GFAP- or nestin-positive cells that extend a single process from SGZ toward the molecular layer. To measure the number of BrdU-labeled RGL

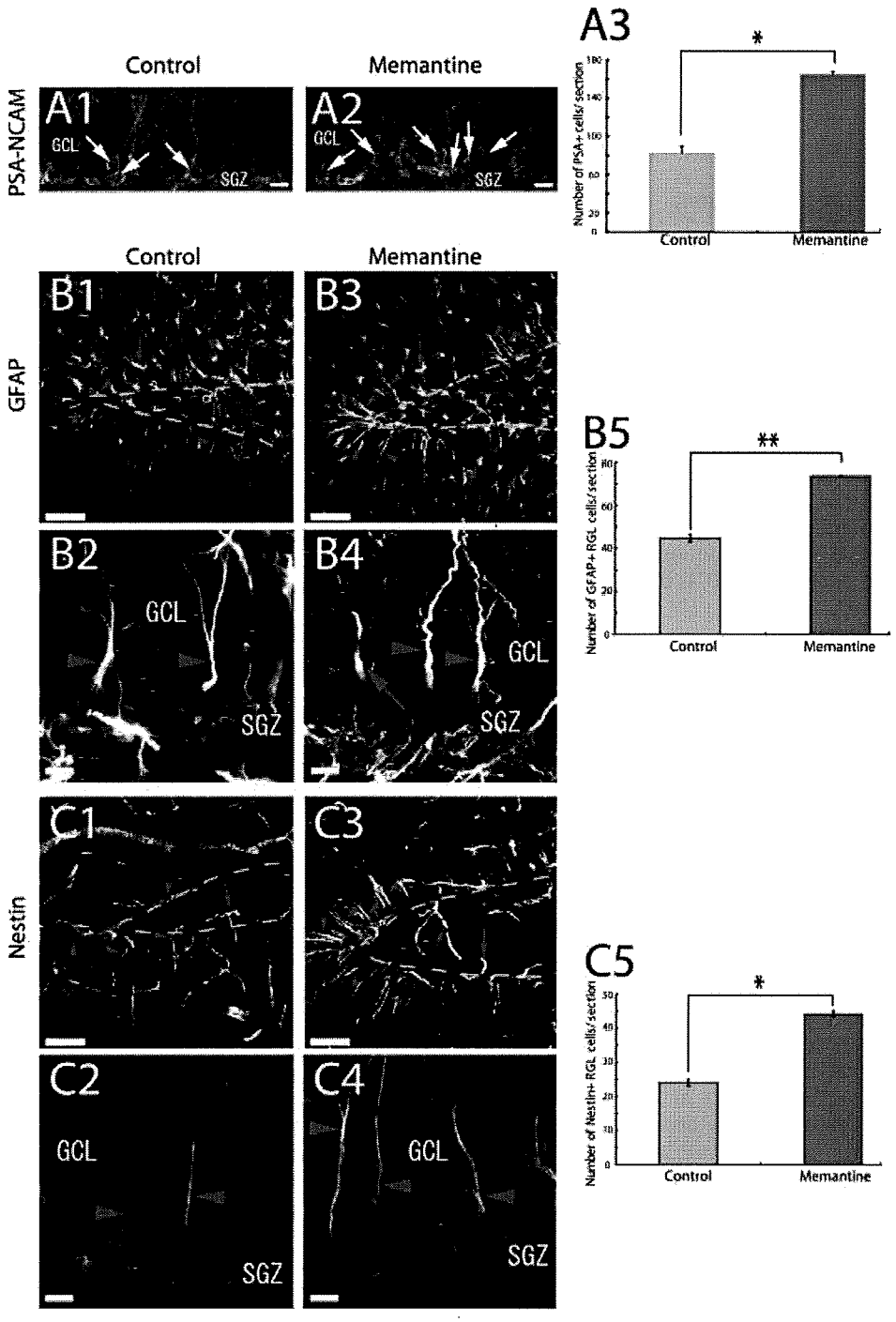

Fig. 1. Effect of memantine on the number of immature neurons and RGL progenitor cells in the DG. Example of immunohistochemical staining with anti-PSA-NCAM antibody (**A**), anti-GFAP antibody (**B**), and anti-nestin antibody (**C**) 10 days after the injection of saline as a control (A1, B1-2, and C1-2) or the injection of memantine (A2, B3-4, and C3-4). The arrows in panel A indicate the PSA-NCAM-positive cells. The arrowheads in panels B and C indicate the RGL progenitor cells. The arrows in panels B and C indicate polygonal astrocytes and cell fragments and blood vessels, respectively. The blue dotted lines in panels B and C indicate the border between the GCL and hilus. Scale bars = 10 μm in panel A, B2, B4, C2, and C4, and 50 μm in panels B1, B3, C1, and C3. Quantitative analysis of the number of immature neurons (A3), GFAP-positive RGL progenitor cells (B5), and nestin-positive RGL progenitor cells (C5) in the GCL. $*P < 0.001$ and $**P < 0.0001$, respectively, when compared with the control group.

progenitor cells in the GCL including the SGZ, an average of nine sections per mouse was analyzed (Figs. 2–5). Cell counting was carried out under a CLSM (FV1000).

Cell Alignment Analysis

The mode of cell division was analyzed as described in previous reports (Chenn and McConnell, 1995; Haydar et al., 2003). Briefly, the position of daughter cells was classified as vertical (daughter cells aligned vertically to the axis of the radial glial fiber) or horizontal (daughter cells aligned horizontally to the axis of the radial glial fiber). Cells were counted while viewing the sections through the 60× objective of a CLSM (FV1000).

Statistical Analysis

Data were evaluated using a one-way analysis of variance followed by the post-hoc Scheffe's *F*-test; some of

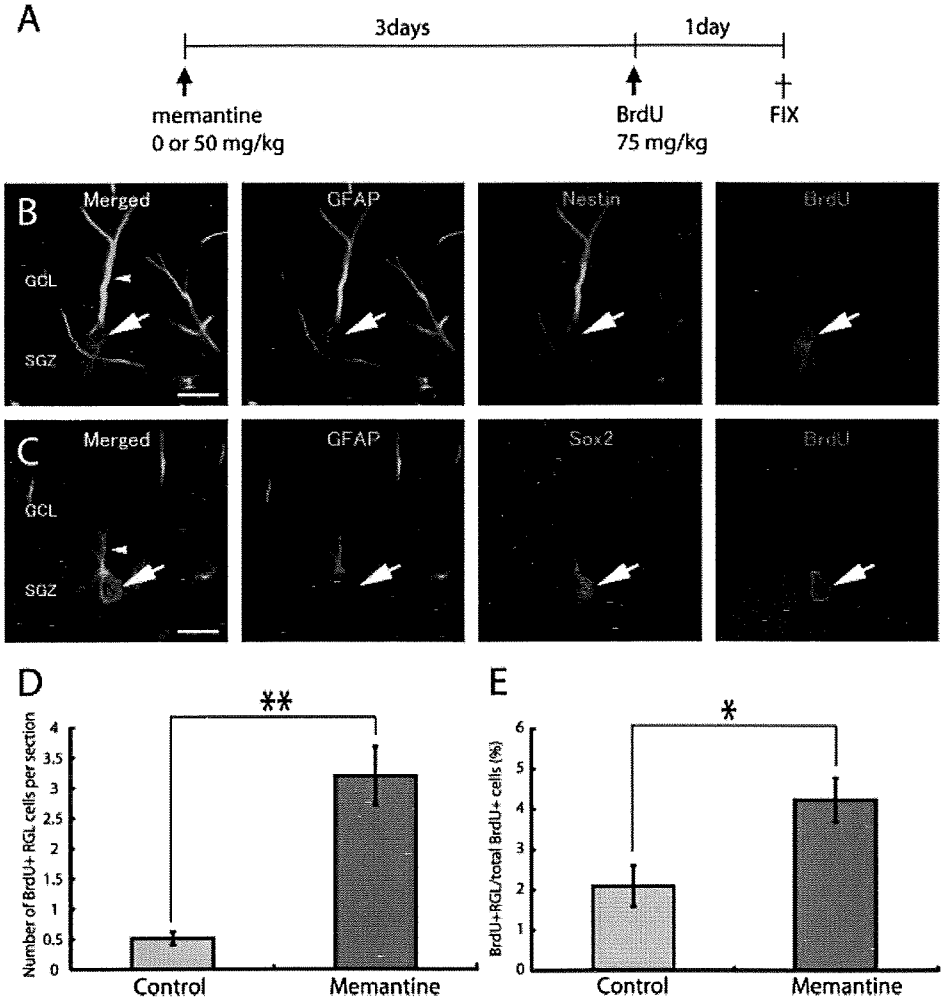

Fig. 2. Immunohistochemical and quantitative analysis of RGL progenitor cells in the GCL 1 day after BrdU-injection. (**A**) Schematic illustration of the experimental design. (**B, C**) Example of BrdU-labeled RGL progenitor cells (arrows) expressing nestin (green) (B) or Sox2 (green) (C) in the memantine-injected group. The arrowheads point to a radial fiber. Scale bar = 10 μm. (**D, E**) Quantitative analysis of the number of BrdU-labeled RGL progenitor cells (D) and the percentage of BrdU-labeled RGL progenitor cells (E) in the GCL. $*P < 0.05$, and $**P < 0.001$, respectively, when compared with the control group.

the data were analyzed using the Mann–Whitney *U*-test. All values were expressed as the mean ± SEM, and *P*-values less than 0.05 were considered significant.

RESULTS

Increase in the Number of RGL Progenitor Cells in Memantine-Injected Mice

To investigate the effect of memantine on the number of RGL progenitor cells in the adult hippocampus, we intraperitoneally injected 3-month-old mice with a dose of 50 mg/kg memantine, fixed their brains 10 days later, and then prepared brain sections. We initially stained the sections with anti-PSA-NCAM antibody, a marker antibody for immature neurons. The number of PSA-NCAM-positive cells in the memantine-injected group was 2.0-fold higher than that in the control group (Fig. 1A; control, 80.3 ± 11.9 cells/section, $n = 3$; memantine, 162.4 ± 25.5 cells/section, $n = 3$), suggesting that memantine promoted neurogenesis in adult mouse hippocampus. We next stained the sections with anti-GFAP antibody and counted the number of GFAP-positive cells with a RGL morphology. The number of GFAP-positive RGL progenitor cells in the memantine-injected group was 1.6-fold higher than that in the control group (Fig. 1B; control, 44.7 ± 9.6 cells/section, $n = 3$; memantine, 73.7 ± 0.25 cells/section, n = 3). In contrast, memantine had no effect on the number or morphology of stellate fibrous GFAP-positive cells in the hilus or molecular layer (data not shown). Similarly, the number of RGL progenitor cells expressing nestin in the memantine-injected group increased by 1.8-fold (Fig. 1C; control, 24.1 ± 3.2 cells/section, $n = 3$; memantine, 44.2 ± 2.52 cells/section, $n = 3$). The greatest increase was observed in the tip of the GCL, where large numbers of progenitor cells are present (Babu et al., 2007). These results indicate that memantine increased the number of RGL progenitor cells in the hippocampus but had no effect on the number or morphology of the stellate fibrous astrocytes.

Memantine Promotes the Proliferation of RGL Progenitor Cells in the GCL

Next, to determine whether the increase in the number of RGL progenitor cells shown in Fig. 1 was due to the proliferation of RGL progenitor cells in response to

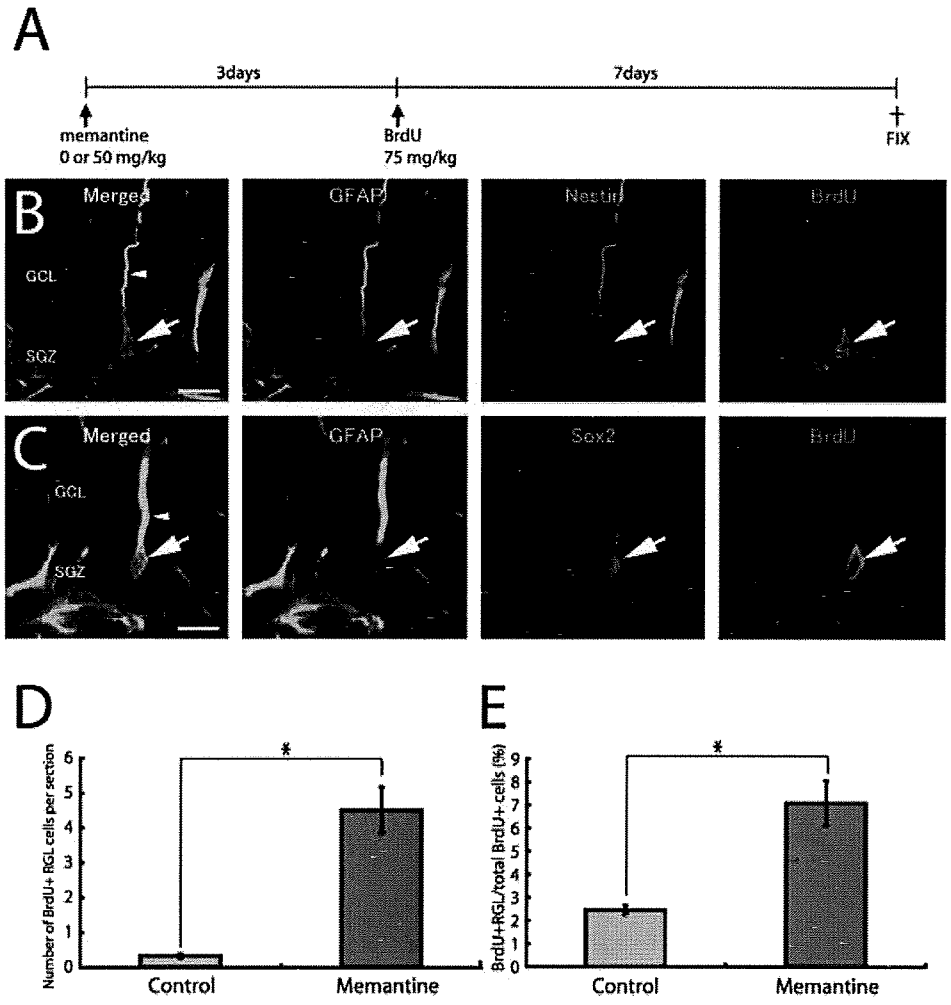

Fig. 3. Immunohistochemical and quantitative analysis of RGL progenitor cells in the GCL 7 days after BrdU-injection. (**A**) Schematic illustration of the experimental design. (**B, C**) Example of BrdU-labeled RGL progenitor cells (arrows) expressing nestin (green) (B) or Sox2 (green) (C) in the memantine-injected group. The arrowheads point to a radial fiber. Scale bar = 10 μm. (**D, E**) Quantitative analysis of the number of BrdU-labeled RGL progenitor cells (D) and the percentage of BrdU-labeled RGL progenitor cells (E) in the GCL. $^{**}P < 0.01$ when compared with the control group.

memantine, we investigated the effect of memantine on the proliferation of RGL progenitor cells. We injected mice with a dose of 50 mg/kg memantine; 3 days later, we injected them with BrdU. Their brains were fixed 1 day after the BrdU-injection (Fig. 2A); after preparing the brain sections, we immunostained them with anti-BrdU antibody and anti-GFAP antibody. In the memantine-injected group, the BrdU-labeled RGL progenitor cells were mainly located in the SGZ and the innermost portion of the GCL (Fig. 2B,C). The staining signals for anti-BrdU antibody were observed in solid or the periphery of the nuclei. Because these staining signals were also observed in previous reports (Nakagawa et al., 2002; Namba et al., 2007), it is unlikely that the different staining signals were caused by the memantine-injection.

The number of BrdU-labeled RGL progenitor cells significantly increased by 5.1-fold in the memantine-injected group (Fig. 2D; control, 0.51 ± 0.11 cells/section, $n = 5$; memantine, 2.59 ± 0.55 cells/section, $n = 5$), and the BrdU-labeled RGL progenitor cells in the memantine-injected group also increased as a percentage of the total BrdU-labeled cells (Fig. 2E; control, 2.09% ± 0.51%, $n = 5$; memantine, 4.23% ± 0.54%, $n = 5$). We then characterized the BrdU-labeled RGL progenitor cells by immunostaining them with two other progenitor cell markers, nestin and Sox2 (Steiner et al., 2006). As shown in Fig. 2B,C, the RGL progenitor cells labeled with BrdU expressed nestin and/or Sox2 as well as GFAP, suggesting that the proliferating RGL progenitor cells possessed the same phenotype as the primary progenitor cells. These findings indicate that memantine significantly increased the proliferation of RGL progenitor cells in the GCL.

Properties of RGL Progenitor Cells Are Maintained Following Memantine-Injection

To further examine the effect of memantine on the fate of the dividing RGL progenitor cells, we injected mice with a dose of 50 mg/kg memantine and 3 days later, we injected them with BrdU; we then fixed their brains 7 days after the BrdU-injection (Fig. 3A). Next, we prepared brain sections and immunostained them with anti-BrdU antibody and anti-GFAP antibody. The number of BrdU-labeled cells with an RGL morphology

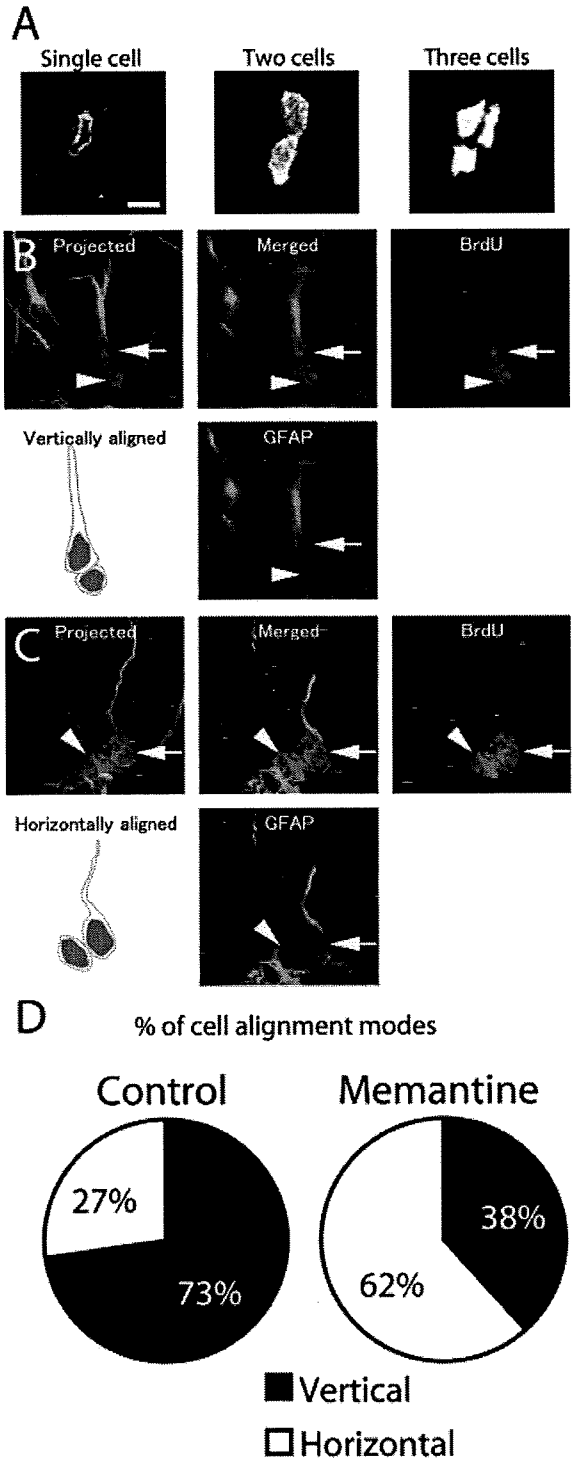

Fig. 4. Cell alignment analysis of BrdU-labeled RGL progenitor cells in the GCL. (**A**) Example of cell clusters one day after BrdU-injection. Scale bar = 10 μm. (**B**) Example of vertically aligned BrdU-labeled RGL progenitor cells (arrow) and non-RGL cells (arrowhead). Both BrdU-labeled cells (red) expressed GFAP (green). (**C**) Example of horizontally aligned BrdU-labeled RGL progenitor cells (arrow) and non-RGL cells (arrowhead). Both BrdU-labeled cells (red) expressed GFAP (green). (**D**) Quantitative analysis of the cell alignment modes in the control group and the memantine-injected group. There was a significant difference ($P < 0.01$) in the cell alignment modes between the control group and the memantine-injected group.

in the GCL dramatically increased by 13.7-fold in the memantine-injected group (Fig. 3D; control, 0.33 ± 0.06 cells/section, $n = 3$; memantine, 4.52 ± 0.66 cells/section, $n = 3$), and the percentage of BrdU-labeled RGL progenitor cells among the total BrdU-labeled cells also increased in the memantine-treated group (Fig. 3E; control, 2.45% ± 0.19%, $n = 3$; memantine, 7.08% ± 0.97%, $n = 3$). Moreover, these BrdU-labeled RGL progenitor cells located in the GCL also expressed the progenitor markers nestin and/or Sox2 (Fig. 3B,C). These findings indicate that a certain number of the divided RGL progenitor cells in the memantine-injected group retained their progenitor properties at least 1 week after cell division.

Memantine Stimulates Symmetric Division of RGL Progenitor Cells in the GCL

Neurogenesis is thought to occur as a result of several modes of cell division. Two examples of these modes are asymmetric cell division, which results in a single daughter neuron and a mother cell that remains a progenitor cell, and symmetric cell division, which expands the pool of progenitor cells (Kriegstein et al., 2006). Recent reports have shown that the mother cell of vertically aligned cells had undergone asymmetric cell division, whereas the mother cell of horizontally aligned cells had undergone symmetric cell division (Encinas et al., 2006; Haydar et al., 2003). To investigate the effect of memantine on the mode of cell division, we examined the alignment of the newly generated pairs of RGL progenitor cells in the GCL 1 day after BrdU-injection. At 1 day after the BrdU-injection, some of the BrdU-labeled cells had formed cell clusters. We divided the cell clusters into three groups based on the number of BrdU-labeled cells in the cell clusters (Fig. 4A) and examined the percentages of these three groups: single cell (control, 40.3% ± 1.6%, $n = 3$; memantine, 35.3% ± 2.5%, $n = 3$), two-cell cluster (control, 29.9% ± 2.0%, $n = 3$; memantine, 29.8% ± 1.8%, $n = 3$), and cluster of three or more cells (control, 29.4% ± 3.1%, $n = 3$; memantine, 34.9% ± 1.9%, $n = 3$). These results indicate that there were no significant differences in the percentages of the three groups between the control and the memantine-injected groups. To investigate the cell alignment modes, we focused on the two-cell clusters with BrdU- and GFAP-positive RGL cells (Fig. 4B,C). More than half of the BrdU-labeled RGL progenitor cells were horizontally aligned in the memantine-injected group (vertical: 38.3%, horizontal: 61.7%), whereas most of the BrdU-labeled RGL progenitor cells in the control group were vertically aligned (vertical: 72.7%, horizontal: 27.3%) (Fig. 4D), suggesting that memantine predominantly stimulates the symmetric division of RGL progenitor cells in the GCL. To further confirm the fate of the RGL progenitor cells, we examined the phenotype of the BrdU-labeled RGL cells in two-cell clusters 2 days after the BrdU-injection in the memantine-injected mice. More than half of the horizontally aligned two-cell

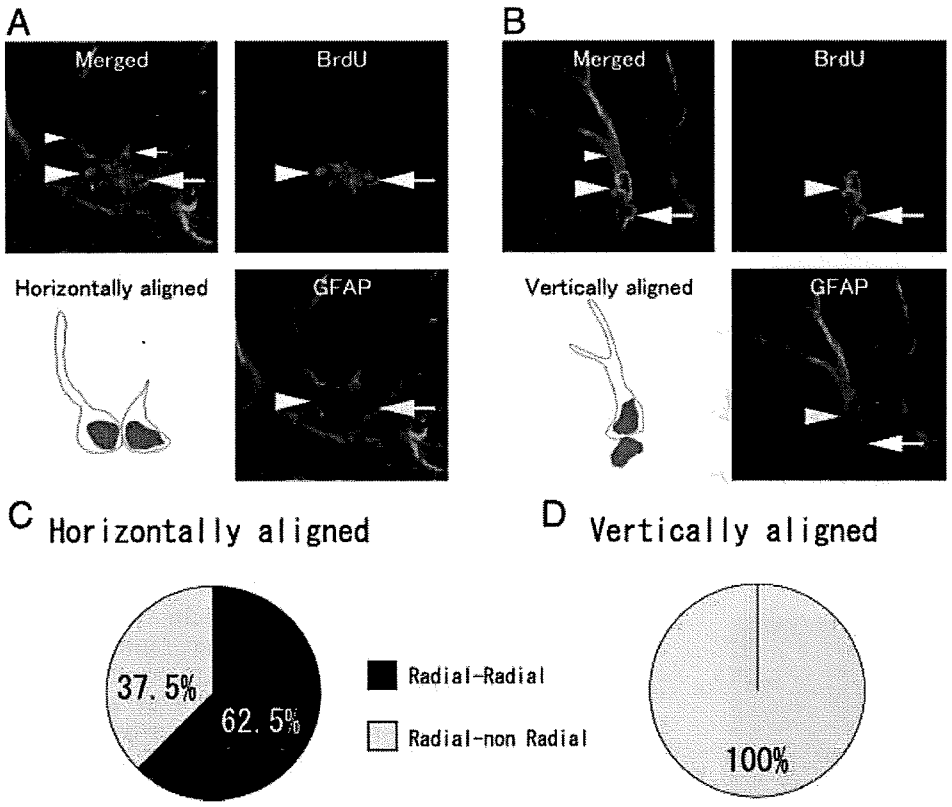

Fig. 5. Phenotype of BrdU-labeled cells in two-cell clusters in memantine-injected mice. (**A**) Example of horizontally aligned BrdU-labeled RGL progenitor cells. One RGL progenitor cell (arrowhead) possesses a long radial process (small arrowhead) and another RGL progenitor cell (arrow) has extended a short process (small arrow). Both BrdU-labeled cells (red) expressed GFAP (green). (**B**) Example of vertically aligned BrdU-labeled RGL progenitor cell (arrowhead) and non-RGL progenitor cell (arrow). The small arrowhead points to the radial process. The BrdU-labeled (red) RGL progenitor cells expressed GFAP (green), but the non-RGL progenitor cells only weakly expressed or did not express GFAP. (**C, D**) Quantitative analysis of the phenotype of BrdU-labeled cells in two-cell clusters.

clusters were formed by two RGL progenitor cells that strongly expressed GFAP (Fig. 5A,C, 62.5%, $n = 3$), suggesting a symmetric fate. In this case, one cell possessed a long radial process and another cell had a short process toward the GCL. This observation suggests that the cells had started to extend their radial processes and to become RGL cells. In contrast, almost all the vertically aligned, two-cell clusters were formed by the RGL progenitor cells and the non-RGL progenitor cells (Fig. 5B,D). The RGL progenitor cell strongly expressed GFAP, whereas the non-RGL progenitor cells weakly expressed or did not express GFAP, suggesting an asymmetric fate. No vertically aligned two-cell clusters formed by two RGL progenitor cells were observed in the present study. Taken together with the findings shown in Figs. 4 and 5, memantine probably enhances the symmetric division of RGL progenitor cells.

DISCUSSION

Neurogenesis in the hippocampus persists throughout life, and the principal source of newly generated neurons is RGL progenitor cells (primary progenitor cells) that express GFAP and/or nestin (Garcia et al., 2004; Lagace et al., 2007; Seki et al., 2007; Seri et al., 2001, 2004). Previous studies have shown that neurogenesis in the adult hippocampus is increased by NMDA-R antagonists, including MK-801 and CGP-43487 (Cameron et al., 1995; Nacher et al., 2001), but the effect of NMDA-R antagonists on RGL progenitor cells was not thoroughly investigated. In the present study, we showed that memantine, an uncompetitive NMDA-R antagonist, had increased the number of BrdU-labeled RGL progenitor cells 1 day after BrdU-injection, indicating that memantine promoted the proliferation of the RGL progenitor cells. Moreover, both the RGL morphology and the expressions of the progenitor cell markers nestin and Sox2 were sustained in the memantine-injected group for as long as 7 days after the BrdU-injection, suggesting that the properties of the progenitor cells were maintained in the newly generated cells following memantine-injection. In consequence, the number of the RGL cells in DG was increased by memantine-injection. This result is supported by the previous study, showing that a competitive NMDA-R antagonist CGP-43487 increased the number of nestin-expressing cells in the adult DG (Nacher et al., 2001). Memantine also affected the mode of cell division by the RGL progenitor cells, because the ratio of horizontally aligned RGL progenitor cells in the memantine-injected group increased significantly in comparison with that in the control group. Recent studies have shown that the alignment of daughter cells is important for determining their fate in the embryonic neocortex (Chenn and McConnell, 1995; Haydar et al., 2003), with horizontally aligned cells appearing to have a symmetric fate and vertically aligned cells appearing to have an asymmetric fate. If this is also the case in the adult hippocampus (Encinas et al., 2006; Kempermann et al., 2004), memantine appears to increase the proportion of

symmetric division in RGL progenitor cells. Taken together with the results of the present study, memantine appears to increase the population of RGL progenitor cells by promoting proliferation through the symmetric division of RGL progenitor cells. This effect of memantine on the primary progenitor cells is unique: memantine induces the expansion of the primary progenitor cell pool, because other stimulations of enhancing neurogenesis such as antidepressants, running, and enriched environment could not increase the number of the primary progenitor cells (Encinas et al., 2006; Kronenberg et al., 2003).

Despite cumulative evidence that NMDA-R antagonists promote neurogenesis, whether functional NMDA receptors are expressed in RGL progenitor cells remains controversial. Although immunohistochemical analyses in recent studies have demonstrated the expression of the NR1 and NR2B subunits of the NMDA-R in primary progenitor cells (Nacher et al., 2007), an electrophysiological study showed that the primary progenitor cells failed to respond to NMDA (Tozuka et al., 2005), indicating that the NR1 and NR2B subunits expressed in the RGL progenitor cells do not form functional NMDA-R. Consequently, it was speculated that NMDA antagonists may inhibit the neuronal activities evoked by glutamate in mature neurons and that the subsequent effects may promote the proliferation of RGL progenitor cells and neurogenesis. One potential candidate affecting the cell proliferation enhanced by memantine is FGF2, a mitogen for neural stem cells (Reynolds and Weiss, 1992). Using quantitative RT-PCR, we found that the expression of FGF2 in the GCL transiently increased by 3.7-fold on 1 day after the memantine-injection but decreased to the basal level on 2 days after the memantine-injection, whereas the expression of EGF, another major mitogen, was not affected by memantine-injection (Supp. Info. Fig. 1). These findings suggest that memantine stimulates the proliferation of RGL progenitor cells via FGF2 signaling. Further studies are needed to elucidate the mechanisms of the up-regulation of FGF2 expression by memantine-injection.

Memantine has been used clinically as a neuroprotective agent for moderate-to-severe Alzheimer's disease but has not been associated with the adverse effects, such as psychotomimetic and cardiovascular effects, shown by other NMDA-R antagonists (Johnson and Kotermanski, 2006; Reisberg et al., 2003). Jin et al. (2006) found that the administration of a clinical dose of memantine in mice (7.5 mg/kg via an intragastric route daily for 2 weeks) increased cell proliferation, and we recently confirmed that most of the newly generated cells in a group of mice injected with memantine ultimately differentiated into mature granule neurons (Maekawa et al., unpublished observations). These results suggest that the promotion of neurogenesis contributes to the therapeutic efficacy of memantine.

In conclusion, we have demonstrated that memantine significantly increases the number of RGL progenitor cells by stimulating symmetric division and that memantine enables the properties of RGL progenitor cells to be maintained in a certain number of newly generated cells, resulting in the expansion of the primary progenitor cell pool in the adult hippocampus.

ACKNOWLEDGMENT

We thank Dr. Tatsunori Seki for his kind gift of the anti-PSA-NCAM antibody.

REFERENCES

Abrous DN, Koehl M, Le Moal M. 2005. Adult neurogenesis: From precursors to network and physiology. Physiol Rev 85:523–569.

Altman J, Das GD. 1965. Autoradiographic and histological evidence of postnatal hippocampal neurogenesis in rats. J Comp Neurol 124:319–335.

Babu H, Cheung G, Kettenmann H, Palmer TD, Kempermann G. 2007. Enriched monolayer precursor cell cultures from micro-dissected adult mouse dentate gyrus yield functional granule cell-like neurons. PLoS ONE 2:e388.

Becker S, Wojtowicz JM. 2007. A model of hippocampal neurogenesis in memory and mood disorders. Trends Cognit Sci 11:70–76.

Cameron HA, McEwen BS, Gould E. 1995. Regulation of adult neurogenesis by excitatory input and NMDA receptor activation in the dentate gyrus. J Neurosci 15:4687–4692.

Chenn A, McConnell SK. 1995. Cleavage orientation and the asymmetric inheritance of Notch1 immunoreactivity in mammalian neurogenesis. Cell 82:631–641.

Doetsch F, Caille I, Lim DA, Garcia-Verdugo JM, Alvarez-Buylla A. 1999. Subventricular zone astrocytes are neural stem cells in the adult mammalian brain. Cell 97:703–716.

Encinas JM, Vaahtokari A, Enikolopov G. 2006. Fluoxetine targets early progenitor cells in the adult brain. Proc Natl Acad Sci USA 103:8233–8238.

Eriksson PS, Perfilieva E, Bjork-Eriksson T, Alborn AM, Nordborg C, Peterson DA, Gage FH. 1998. Neurogenesis in the adult human hippocampus. Nat Med 4:1313–1317.

Filippov V, Kronenberg G, Pivneva T, Reuter K, Steiner B, Wang LP, Yamaguchi M, Kettenmann H, Kempermann G. 2003. Subpopulation of nestin-expressing progenitor cells in the adult murine hippocampus shows electrophysiological and morphological characteristics of astrocytes. Mol Cell Neurosci 23:373–382.

Fukuda S, Kato F, Tozuka Y, Yamaguchi M, Miyamoto Y, Hisatsune T. 2003. Two distinct subpopulations of nestin-positive cells in adult mouse dentate gyrus. J Neurosci 23:9357–9366.

Garcia AD, Doan NB, Imura T, Bush TG, Sofroniew MV. 2004. GFAP-expressing progenitors are the principal source of constitutive neurogenesis in adult mouse forebrain. Nat Neurosci 7:1233–1241.

Haydar TF, Ang E Jr, Rakic P. 2003. Mitotic spindle rotation and mode of cell division in the developing telencephalon. Proc Natl Acad Sci USA 100:2890–2895.

Hirasawa T, Wada H, Kohsaka S, Uchino S. 2003. Inhibition of NMDA receptors induces delayed neuronal maturation and sustained proliferation of progenitor cells during neocortical development. J Neurosci Res 74:676–687.

Jin K, Xie L, Mao XO, Greenberg DA. 2006. Alzheimer's disease drugs promote neurogenesis. Brain Res 1085:183–188.

Johnson JW, Kotermanski SE. 2006. Mechanism of action of memantine. Curr Opin Pharmacol 6:61–67.

Kee N, Teixeira CM, Wang AH, Frankland PW. 2007. Preferential incorporation of adult-generated granule cells into spatial memory networks in the dentate gyrus. Nat Neurosci 10:355–362.

Kempermann G, Jessberger S, Steiner B, Kronenberg G. 2004. Milestones of neuronal development in the adult hippocampus. Trends Neurosci 27:447–452.

Kriegstein A, Noctor S, Martinez-Cerdeno V. 2006. Patterns of neural stem and progenitor cell division may underlie evolutionary cortical expansion. Nat Rev Neurosci 7:883–890.

Kronenberg G, Reuter K, Steiner B, Brandt MD, Jessberger S, Yamaguchi M, Kempermann G. 2003. Subpopulations of proliferating cells of the adult hippocampus respond differently to physiologic neurogenic stimuli. J Comp Neurol 467:455–463.

Kuhn HG, Dickinson-Anson H, Gage FH. 1996. Neurogenesis in the dentate gyrus of the adult rat: Age-related decrease of neuronal progenitor proliferation. J Neurosci 16:2027–2033.

Lagace DC, Whitman MC, Noonan MA, Ables JL, DeCarolis NA, Arguello AA, Donovan MH, Fischer SJ, Farnbauch LA, Beech RD, DiLeone RJ, Greer CA, Mandyam CD, Eisch AJ. 2007. Dynamic contribution of nestin-expressing stem cells to adult neurogenesis. J Neurosci 27:12623–12629.

Liu J, Solway K, Messing RO, Sharp FR. 1998. Increased neurogenesis in the dentate gyrus after transient global ischemia in gerbils. J Neurosci 18:7768–7778.

Maekawa M, Takashima N, Arai Y, Nomura T, Inokuchi K, Yuasa S, Osumi N. 2005. Pax6 is required for production and maintenance of progenitor cells in postnatal hippocampal neurogenesis. Genes Cells 10:1001–1014.

Nacher J, Rosell DR, Alonso-Llosa G, McEwen BS. 2001. NMDA receptor antagonist treatment induces a long-lasting increase in the number of proliferating cells, PSA-NCAM-immunoreactive granule neurons and radial glia in the adult rat dentate gyrus. Eur J Neurosci 13:512–520.

Nacher J, Varea E, Miguel Blasco-Ibanez J, Gomez-Climent MA, Castillo-Gomez E, Crespo C, Martinez-Guijarro FJ, McEwen BS. 2007. *N*-methyl-D-aspartate receptor expression during adult neurogenesis in the rat dentate gyrus. Neuroscience 144:855–864.

Nakagawa S, Kim JE, Lee R, Malberg JE, Chen J, Steffen C, Zhang YJ, Nestler EJ, Duman RS. 2002. Regulation of neurogenesis in adult mouse hippocampus by cAMP and the cAMP response element-binding protein. J Neurosci 22:3673–3682.

Namba T, Mochizuki H, Onodera M, Mizuno Y, Namiki H, Seki T. 2005. The fate of neural progenitor cells expressing astrocytic and radial glial markers in the postnatal rat dentate gyrus. Eur J Neurosci 22:1928–1941.

Namba T, Mochizuki H, Onodera M, Namiki H, Seki T. 2007. Postnatal neurogenesis in hippocampal slice cultures: Early in vitro labeling of neural precursor cells leads to efficient neuronal production. J Neurosci Res 85:1704–1712.

Parent JM, Yu TW, Leibowitz RT, Geschwind DH, Sloviter RS, Lowenstein DH. 1997. Dentate granule cell neurogenesis is increased by seizures and contributes to aberrant network reorganization in the adult rat hippocampus. J Neurosci 17:3727–3738.

Reisberg B, Doody R, Stoffler A, Schmitt F, Ferris S, Mobius HJ. 2003. Memantine in moderate-to-severe Alzheimer's disease. N Engl J Med 348:1333–1341.

Reynolds BA, Weiss S. 1992. Generation of neurons and astrocytes from isolated cells of the adult mammalian central nervous system. Science 255:1707–1710.

Schmidt-Hieber C, Jonas P, Bischofberger J. 2004. Enhanced synaptic plasticity in newly generated granule cells of the adult hippocampus. Nature 429:184–187.

Seki T, Arai Y. 1991. Expression of highly polysialylated NCAM in the neocortex and piriform cortex of the developing and the adult rat. Anat Embryol (Berl) 184:395–401.

Seki T, Arai Y. 1993. Highly polysialylated neural cell adhesion molecule (NCAM-H) is expressed by newly generated granule cells in the dentate gyrus of the adult rat. J Neurosci 13:2351–2358.

Seki T, Arai Y. 1995. Age-related production of new granule cells in the adult dentate gyrus. Neuroreport 6:2479–2482.

Seki T, Namba T, Mochizuki H, Onodera M. 2007. Clustering, migration, and neurite formation of neural precursor cells in the adult rat hippocampus. J Comp Neurol 502:275–290.

Seri B, Garcia-Verdugo JM, Collado-Morente L, McEwen BS, Alvarez-Buylla A. 2004. Cell types, lineage, and architecture of the germinal zone in the adult dentate gyrus. J Comp Neurol 478:359–378.

Seri B, Garcia-Verdugo JM, McEwen BS, Alvarez-Buylla A. 2001. Astrocytes give rise to new neurons in the adult mammalian hippocampus. J Neurosci 21:7153–7160.

Steiner B, Klempin F, Wang L, Kott M, Kettenmann H, Kempermann G. 2006. Type-2 cells as link between glial and neuronal lineage in adult hippocampal neurogenesis. Glia 54:805–814.

Tozuka Y, Fukuda S, Namba T, Seki T, Hisatsune T. 2005. GABAergic excitation promotes neuronal differentiation in adult hippocampal progenitor cells. Neuron 47:803–815.

van Praag H, Schinder AF, Christie BR, Toni N, Palmer TD, Gage FH. 2002. Functional neurogenesis in the adult hippocampus. Nature 415:1030–1034.

von Bohlen Und Halbach O. 2007. Immunohistological markers for staging neurogenesis in adult hippocampus. Cell Tissue Res 329:409–420.

Wojtowicz JM, Askew ML, Winocur G. 2008. The effects of running and of inhibiting adult neurogenesis on learning and memory in rats. Eur J Neurosci 27:1494–1502.

GLIA

GLIA 58:790–801 (2010)

$P2Y_{12}$ Receptor-Mediated Integrin-β1 Activation Regulates Microglial Process Extension Induced by ATP

KEIKO OHSAWA,[1] YASUHIRO IRINO,[2] TOMOMI SANAGI,[1] YASUKO NAKAMURA,[1] ERI SUZUKI,[1] KAZUHIDE INOUE,[3] AND SHINICHI KOHSAKA[1]*

[1]*Department of Neurochemistry, National Institute of Neuroscience, Kodaira, Tokyo 187-8502, Japan*
[2]*Division of Lipid Biochemistry, Graduate School Medicine, Kobe University, Chuo-ku, Kobe Hyogo, Japan*
[3]*Department of Molecular and System Pharmacology, Graduate School of Pharmaceutical Sciences, Kyushu University, Higashi, Fukuokas, Japan*

KEY WORDS
chemotaxis; purinergic; adhesion; hippocampus

ABSTRACT
Microglia are the primary immune surveillance cells in the brain, and when activated they play critical roles in inflammatory reactions and tissue repair in the damaged brain. Microglia rapidly extend their processes toward the damaged areas in response to stimulation of the metabotropic ATP receptor $P2Y_{12}$ by ATP released from damaged tissue. This chemotactic response is a highly important step that enables microglia to function properly at normal and pathological sites in the brain. To investigate the molecular pathways that underlie microglial process extension, we developed a novel method of modeling microglial process extension that uses transwell chambers in which the insert membrane is coated with collagen gel. In this study, we showed that ATP increased microglial adhesion to collagen gel, and that the ATP-induced process extension and increase in microglial adhesion were inhibited by integrin blocking peptides, RGD, and a functional blocking antibody against integrin-β1. An immunoprecipitation analysis with an antibody against the active form of integrin-β1 showed that $P2Y_{12}$ mediated the integrin-β1 activation by ATP. In addition, time-lapse imaging of EGFP-labeled microglia in mice hippocampal slices showed that RGD inhibited the directional process extension toward the nucleotide source, and immunohistochemical staining showed that integrin-β1 accumulated in the tips of the microglial processes in rat hippocampal slices stimulated with ADP. These findings indicate that ATP induces the integrin-β1 activation in microglia through $P2Y_{12}$ and suggest that the integrin-β1 activation is involved in the directional process extension by microglia in brain tissue.

INTRODUCTION

Microglia are present in the normal brain as ramified-type cells that have highly branched, motile cell processes. In pathological states in the brain, microglia alter their morphology and migrate toward injured neurons, where they exhibit various kinds of activated functions that lead to repair of damaged tissue (Kreutzberg, 1996; Nakajima and Kohsaka, 2005). Extracellular nucleotides are released from stimulated or injured cells (Burnstock, 2008; Koizumi et al., 2003), and ATP is known to regulate microglial functions through ionotropic (P2Xs) or metabotropic (P2Ys) purinergic receptors (Franke et al., 2006; Inoue, 2006). We have previously reported that ATP induces microglial migration mediated by Gi/o-coupled $P2Y_{12}$ (Honda et al., 2001) and that the migration requires activation of phosphatidylinositol 3′-kinase (PI3K) and phospholipase C (PLC) signaling pathways (Irino et al., 2008; Ohsawa et al., 2007). Recent studies have demonstrated that microglia extend their processes toward a lesion site within minutes of brain damage and that the extension is mediated by $P2Y_{12}$ (Davalos et al., 2005; Haynes et al., 2006; Kurpius et al., 2007; Nimmerjahn et al., 2005). Thus, rapid process extension is the first response of microglia to brain damage and an important step in the process by which microglia adapt their functional activity to environmental changes. Although P2Y-associated outward potassium channels and PI3K pathways have been reported to be involved in the ATP-induced process extension (Wu et al., 2007), the precise signaling pathways underlying microglial process extension are not well understood.

Adhesive interactions with the surrounding extracellular matrix (ECM) are critical determinants of process extension and cell migration, and integrins are a major family of heterodimeric cell adhesion molecules. Thus far, 18 α subunits and eight β subunits have been identified and found to form 24 αβ pairs, and the resulting molecules are divided into three classes: β1, β2, and αv (Hynes, 2002). Microglia express integrins in each of these three classes (Milner and Campbell, 2002a), and expression of specific integrins has been shown to be upregulated following microglial activation in pathological conditions (Bo et al., 1996; Kloss et al., 1999; Tsuda et al., 2003). Recent studies have revealed that integrin-β1 is involved in the ADP-induced migration and proliferation by microglia on fibronectin-coated dishes (Nasu-Tada et al., 2005) and in their engulfment of invading

Additional Supporting Information may be found in the online version of this article.

Grant sponsors: Japanese Ministry of Health, Labour and Welfare, Japanese Ministry of Education, Culture, Sports, Science and Technology.

*Correspondence to: Shinichi Kohsaka. Department of Neurochemistry, National Institute of Neuroscience, 4-1-1 Ogawahigashi, Kodaira, Tokyo 187-8502, Japan. E-mail: kohsaka@ncnp.go.jp

Received 10 September 2009; Accepted 15 December 2009

DOI 10.1002/glia.20963

Published online 20 January 2010 in Wiley InterScience (www.interscience.wiley.com).

polymorphonuclear neutrophils in hippocampal slice cultures following oxygen-glucose deprivation (Neumann et al., 2008). The results of the aforementioned studies suggest that integrins play an important role in activated microglia in pathological states. The molecular mechanisms by which integrins affect the motility of activated microglia are becoming clearer, but their role in microglial process extension is not understood.

To analyze the molecular mechanisms underlying ATP-induced microglial process extension, in this study, we developed a novel *in vitro* assay for microglial process extension and performed time-lapse confocal imaging of microglia expressing EGFP in mice hippocampal slices. The results demonstrate that ATP-stimulated $P2Y_{12}$ induces integrin-β1 activation, which leads to an increase in microglial adhesion, and they suggest that interaction between ATP-activated integrin-β1 and the ECM may regulate the directional process extension by microglia in the brain tissue of the early stage following neuronal injury.

MATERIALS AND METHODS

Cell Culture

Microglia were obtained from primary cell cultures of neonatal Wistar rat cerebral cortex as described previously (Nakajima et al., 1992). In brief, mixed glial cultures were maintained for 12–23 d in DMEM (Invitrogen) supplemented with 10% fetal calf serum (FCS) (Irvine Scientific). Microglia were prepared as floating cells by gentle shaking, and after collecting them, they were allowed to attach to appropriate dishes.

Process Extension Assay

The insert membrane of a transwell chamber (24-plate type, 8.0 μm pores, Corning) were coated with 50 μL of Cellmatrix Type-IA collagen gel (Nitta Gelatin) and washed with serum-free DMEM. Microglia (2×10^5 cells/200 μL) were seeded in serum-free DMEM on the gels, and after incubation for 30 min the cells were washed with serum-free DMEM for 1 h. After leaving 50 μL of medium in each insert, the insert was transferred into a bottom well of the plate containing 600 μL DMEM. After incubation for 10 min, 50 μM ATP (SIGMA) was added to the bottom well, and the cells were incubated for 2 h at 37°C. To fix the cells, 100 μL of PBS containing 8% paraformaldehyde (PFA) was added to each insert, and the medium in the bottom well was replaced with PBS containing 4% PFA. After incubation for 5 min, the cells were additionally fixed with 4% PFA in PBS for 20 min, and then permeabilized for 30 min with 0.1% Triton X-100 in PBS. After blocking in PBS containing 3% BSA, 3% goat serum, and 0.05% Triton X-100 (blocking buffer) for 30 min, the cells were incubated with anti-Iba1 polyclonal antibody (1 μg/mL) (Imai et al., 1996) in blocking buffer for 2 h, and incubated with Alexa Fluor 488-conjugated anti-rabbit IgG (1:1,000; Invitrogen) and Texas Red-conjugated phalloidin (2 units/ml; Invitrogen) for 2 h. Next, the cells were washed with PBS containing 0.05% Triton X-100 and stained with DAPI (1:1,000; DOJINDO Laboratories) in PBS. After washing with PBS, the membranes together with the gels were cut off the inserts and mounted in Vectashield (Vector Laboratories). The morphology of the microglia was examined with an FV1000 confocal laser-scanning microscope (CLSM) (Olympus) and a 40× objective. XY-images were acquired at 2 μm *z*-step intervals between the gel surface and the depths where the tips of the microglial processes were detected in the gels. The integral fluorescence intensity of each XY-image was calculated with FV10-ASW software (Olympus). The XY-image containing microglial cell bodies in the layer just beneath gel surface exhibited the highest integral intensity of Alexa Fluor 488 or Texas-red fluorescence. The integral intensity of the fluorescence in the images gradually decreased as the density of the microglial processes declined. The image in which the integral intensity of Alexa Fluor 488 or Texas-Red fluorescence was 0.01% of its highest intensity was assumed to be the deepest image containing the tips of microglial processes. The distance that the processes had extended was quantified by calculating the distance, *Z*, between the image containing the highest intensity of DAPI fluorescence and the deepest image containing the tips of the microglial processes. We used FITC-conjugated beads to confirm that the fluorescence signals from the gel surface to a depth of 100 μm were detected with 40× objective in the same way. The effects of the inhibitors, peptides, and antibodies were assessed by preincubating cells with AR-C69931MX (AstraZeneca) (1 μM) for 10 min, pyridoxal-phosphate-6-azophenyl-2′,4′-disulfonic acid (PPADS) (Sigma) (100 μM) for 10 min, wortmannin (Sigma) (2 μM) for 10 min, LY294002 (Wako) (50 μM) for 10 min, U73122 and U73343 (Sigma) (100 nM) for 5 min, RGD peptide and RGE peptide (SIGMA) (300 μM) for 30 min, and anti-integrin-β1 antibody (clone Ha2/5, BD Bioscience, #555002), anti-integrin-β3 antibody (clone 2C9.G2, Biolegend, #104309), control hamster IgM (BD Bioscience, #553957) and control hamster IgG (BD Bioscience, #553968) (5 μg/mL) for 1 h, and then stimulating them with ATP.

Cell Adhesion Assay

The culture wells of 48-well plates (Corning) were coated with 200 μL PureCol type I collagen gel (Cosmo Bio) and allowed to stand for 1 h. They were then washed three times with serum-free DMEM. Microglia (2×10^4 cells) were resuspended in 200 μL of DMEM, and ATP or ADP was added to each cell suspension. The cells were seeded on the gels, and after immediately centrifuging the plates at 1,500 rpm for 3 min to attach the cells to the gels, the gels were incubated for 1 h at 37°C. The adhesion assay was stopped by adding 500 μL of DMEM to each well and washing off the loosely attached cells. The attached cells were fixed with 4% PFA in PBS for 20 min and then washed with PBS. The cells were permeabilized

for 5 min with 0.1% Triton X-100 in PBS, and then stained with 0.3% Toluidine Blue. We counted the number of cells in three random areas under a microscope and a 10× objective, and calculated the average number of cells per 1 mm^2. The results were expressed as the ratio of the number of cells that had adhered under stimulated conditions to the number that had adhered under unstimulated conditions. Each experiment was performed in duplicate. The data reported were the means ± SEM of the data obtained in three experiments. In the peptide and antibody-blocking experiments, the suspension of cells was incubated with the peptide or antibody for 10 min before stimulation with ATP or ADP. The RGD peptide and RGE peptide were used at a concentration of 30 μM, and the monoclonal antibodies against integrin-β1 and integrin-β3 and isotype controls were used at a concentration of 10 μg/mL.

Measurement of Integrin-β1 Activity by Immunoprecipitation

Integrin-β1 activity was measured by immunoprecipitation as described previously (Oinuma et al., 2006). Human astrocytoma 1321N1 cells do not express any detectable endogenous receptor for adenine nucleotides (Filtz et al., 1994), and both ATP and ADP have been reported to be agonists of rat $P2Y_{12}$ heterologously expressed in 1321N1 cells (Simon et al., 2002). To study signaling pathways downstream of $P2Y_{12}$, we prepared 1321N1 cells stably expressing HA-tagged rat $P2Y_{12}$ (1321N1-P2Y12), and the results confirmed that ATP activates the PI3K-Akt signaling pathway through $P2Y_{12}$ in 1321N1-P2Y12 cells (Supp. Info. Fig. 2). The 1321N1 cells were maintained in DMEM (low-glucose type) (DMEM-L; Invitrogen) supplemented with 10% FCS, and the 1321N1-P2Y12 cells were cultured in DMEM-L supplemented with 10% FCS plus 1.5 mg/mL geneticin sulfate (Invitrogen). To collect intact cells without enzyme processing, 1321N1 cells and 1321N1-P2Y12 cells were cultured on RepCell temperature-responsive dishes (CellSeed) for 1 day. The cells were then washed with PBS and incubated in PBS containing 1 mM EDTA for 30 min at room temperature (RT). Detached cells were washed and resuspended in serum-free DMEM-L, and after plating them onto dishes coated with Cellmatrix collagen gel, they were stimulated with 100 μM ATP. The cells were lysed directly on the dishes with ice-cold lysis buffer (50 mM Tris-HCl pH 7.4, 150 mM NaCl, 1 mM Na_3VO_4, 25 mM NaF, 10%[v/v] Glycerol, 1%[v/v] Triton X-100) supplemented with a protease inhibitor cocktail (Roche) and phosphatase inhibitor cocktail PhosSTOP (Roche). The lysates were clarified by centrifugation for 10 min, and 30 μL of each supernatant was mixed with SDS-sample buffer to measure the total level of integrin-β1 in the cell lysate, and the remaining supernatants were used as the cell lysates for immunoprecipitation. The cell lysates were incubated for 2 h at 4°C with 2 μg of an antibody that recognizes the active form of integrin-β1 (HUTS-4, Millipore) and incubated for 1 h at 4°C with protein G-sepharose beads (GE Healthcare). The beads were then washed twice with lysis buffer, and the bound proteins were eluted in SDS-sample buffer.

The cell lysates and the immunoprecipitatd samples were subjected to 10% SDS-PAGE and transferred onto an Immobilon P membrane (Millipore). The membrane was incubated for 1 h at RT with a blocking solution containing 25 mM Tris, pH 7.5, 150 mM NaCl, 0.1%(v/v) Tween 20 (TTBS), and 5% (v/v) nonfat dry milk, and then incubated overnight at 4°C with mouse monoclonal antibody against integrin-β1 (clone 18, 1:250; BD Biosciences). Next, the membrane was incubated for 1 h at room temperature with horseradish peroxidase (HRP)-conjugated donkey anti-mouse IgG (1:1,000; GE Healthcare), and integrin-β1 was detected with an ECL Western blotting detection system (GE Healthcare).

Immunohistochemistry

Adult rats were anesthetized and then perfused transcardially with 4% PFA in PBS. Brains were dissected and postfixed at 4°C overnight. The brains were immersed in 20% sucrose in PBS, embedded in optimal cutting temperature (OTC) compound (Sakura Finetechnical), and frozen in dry ice. The frozen brains were cut into 20 μm sections with a cryostat CM-3000 (Leica), and the sections were then mounted onto 3-aminopropyltriethoxysilane (APS)-coated glass slides (Matsunami). After permeabilizing the sections with 0.1% Triton X-100 in PBS and blocking them with 10% goat serum-0.05% Triton X-100 in PBS for 30 min, they were incubated overnight at 4°C with 5 μg/mL of hamster monoclonal anti-integrin-β1 antibody (clone Ha2/5) or control hamster IgM. Following three washes with 0.05% Triton X-100 in PBS, the sections were incubated for 4 h at RT with mouse monoclonal anti-hamster IgM antibody (2 μg/mL) (BD Biosciences) and rabbit polyclonal anti-Iba1 antibody (1 μg/mL) in PBS containing 1% goat serum-0.05% Triton X-100. After washes, the sections were incubated with Alexa Fluor488-goat anti-mouse IgG (1:1,000; Invitrogen) and Alexa Fluor594-goat anti-rabbit IgG (1:1,000; Invitrogen), and after washing again, the sections were stained with DAPI in PBS and then mounted on a glass slide with Vectashield. Fluorescent images were taken with FV1000 confocal laser-scanning microscope and a 60× objective.

Hippocampal Slice Culture and Time-Lapse Imaging of Microglia

We used the hippocampal slice system as described previously (Kurpius et al., 2006) to examine microglial behavior following ADP application to the bath. To immunohistochemically stain microglia, we prepared hippocampal tissue slices from 4- to 8-day-old rats. For time-lapse imaging of microglia, we used 4- to 7-day-old Iba1-EGFP transgenic mice and visualized their

microglia by EGFP fluorescence (Hirasawa et al., 2005). Brains were removed in ice-cold Hank's balanced salt solution (HBSS, Invitrogen) supplemented with dextrose (6 mg/mL), and then sectioned transversely (400 μm thick slices) with a tissue chopper (The Mickle Laboratory Engineering). The slices were incubated for 1 h in oxygenated culture medium (Modified Eagle Medium [MEM] containing 25 mM HEPES, pH 7.4, 2 mM glutamine, 20 U/ml penicillin, and 20 μg/ml streptomycin). The slice was placed at the center of a specimen chamber and covered carefully with a piece of filter membrane (1-μm pore size), and the edge of the membrane was attached to the coverslip with cyanoacrylate glue. Oxygenated culture medium (500 μL) was then added to the chamber well, and the chamber was placed on the stage of an IX81 microscope (Olympus) in a small incubator (Olympus) which is warmed to 36°C and contained an atmosphere composed of 95% O_2 and 5% CO_2. Following the addition of 1 mM ADP to the culture medium in the chamber, a series of sets of images of microglia expressing EGFP were taken at 5-min intervals for 1 h through an FV1000 confocal laser scanning microscope and a 20× objective. Each set of images in the series consisted of 20 *z*-steps spaced 2 μm apart to a total depth of 40 μm and maximum projection of EGFP signals is reconstructed by stacking XY-images in the direction of the *Z*-axis. Image processing and analysis was performed with Image-Pro Plus software (Media Cybernetics) To examine the effect of peptides on microglial motility, the slices were incubated for 1 h in culture medium containing 1 mM RGE peptide or 1 mM RGD peptide and then placed on the chamber in culture medium containing each peptide.

RESULTS

ATP Induces $P2Y_{12}$-Mediated Process Extension by Primary-Culture Microglia in Collagen Gels

To examine the molecular signaling pathways that regulate ATP-induced process extension by microglia, we first used Transwell chambers containing collagen gel in their insert well to establish an *in vitro* assay system. Primary-culture microglia were plated on the gel in each insert well, and ATP was added to the bottom well (Fig. 1A). After incubation for 2 h, cells on and in the gel were fixed and then stained with DAPI, anti-Iba1 antibody, and Texas-Red conjugated phalloidin, and the morphology of the Iba1-immunopositive cells in the gels was examined with a confocal laser microscope. To confirm the formation of an ATP gradient in the gels, we applied fluorescent BodipyTR-ATP into the bottom well. Confocal images of fluorescent signals in the gels showed that a three-dimensional ATP gradient was rapidly established in the gels and maintained for several hours (Supp. Info. Fig. 1). Within 30 min after 50 μM ATP stimulation, Iba1-positive cells began to extend processes into the gels, and at 2 h cells extended long, highly branched processes into the gels toward the ATP while their cell bodies remained on the surface of the gels (Fig. 1B–E). In the absence of the addition of ATP, most of the cells were detached from gels by washing, and the cells remaining on the gels were round and had not sent out any processes into the gels. When 50 μM ATP was simultaneously added to both the bottom well and the insert well, the microglia extended lamellipodia- or microspike-like processes in random directions along the surface of the gels, but most of the cells did not extend processes into the gels. These results demonstrate that the extension of processes by microglia is dependent on the ATP concentration gradient in the gel. A $P2Y_{12}$ agonist, ADP, induced process extension the same as ATP did, but neither UTP nor UDP, which are a $P2Y_1$ and $P2Y_2$ agonist and a $P2Y_6$ agonist, respectively, did (Fig. 2A). A $P2Y_{12}$ selective antagonist, AR-C69931MX, inhibited process extension, but PPADS, which is an antagonist of $P2Y_1$, $P2Y_2$, and $P2Y_6$, had no effect. These results indicate that $P2Y_{12}$ mediates the process extension by microglia in gels.

Inhibitors of PI3K and PLC Block ATP-Induced Process Extension by Microglia

We have previously reported that $P2Y_{12}$-mediated activation of PI3K and PLC signaling pathways is required for microglial migration in response to ATP (Irino et al., 2008; Ohsawa et al., 2007). To investigate the involvement of PI3K and PLC in the ATP-induced process extension by microglia, we examined the effect of two PI3K inhibitors, wortmannin and LY294002, and a PLC inhibitor, U73122, on process extension. As shown in Fig. 2B, pretreatment with wortmannin (2 μM) or LY294002 (50 μM) significantly inhibited the process extension by microglia. The PLC inhibitor U73312 (100 nM) completely blocked process extension; however, a negative control analogue, U73343 (100 nM), had no effect. These results suggest that activation of PI3K and PLC are required for process extension.

RGD and a Functional-Blocking Antibody of Integrin-β1 Inhibit ATP-Induced Process Extension by Microglia

As shown in Fig. 1C, almost all of the unstimulated microglia were detached from the gels by washing, whereas most of the ATP-stimulated cells remained attached to the gels. These observations suggested that the adhesion of naïve microglia to collagen gels is weak and that ATP strengthens the interaction between microglia and collagen. Integrins are a large family of cell surface receptors for ECM and have been found to regulate process extension and cell migration. To determine whether integrins contribute to ATP-induced process extension by microglia, we pretreated microglial cells with integrin inhibiting RGD peptide. Pretreatment with RGD peptides (300 μM) significantly suppressed process extension, and negative control RGE peptide had no effect (Fig. 3A). Furthermore, to identify the integrin subtypes that participate in process extension, we examined the effects of functional blocking antibodies against

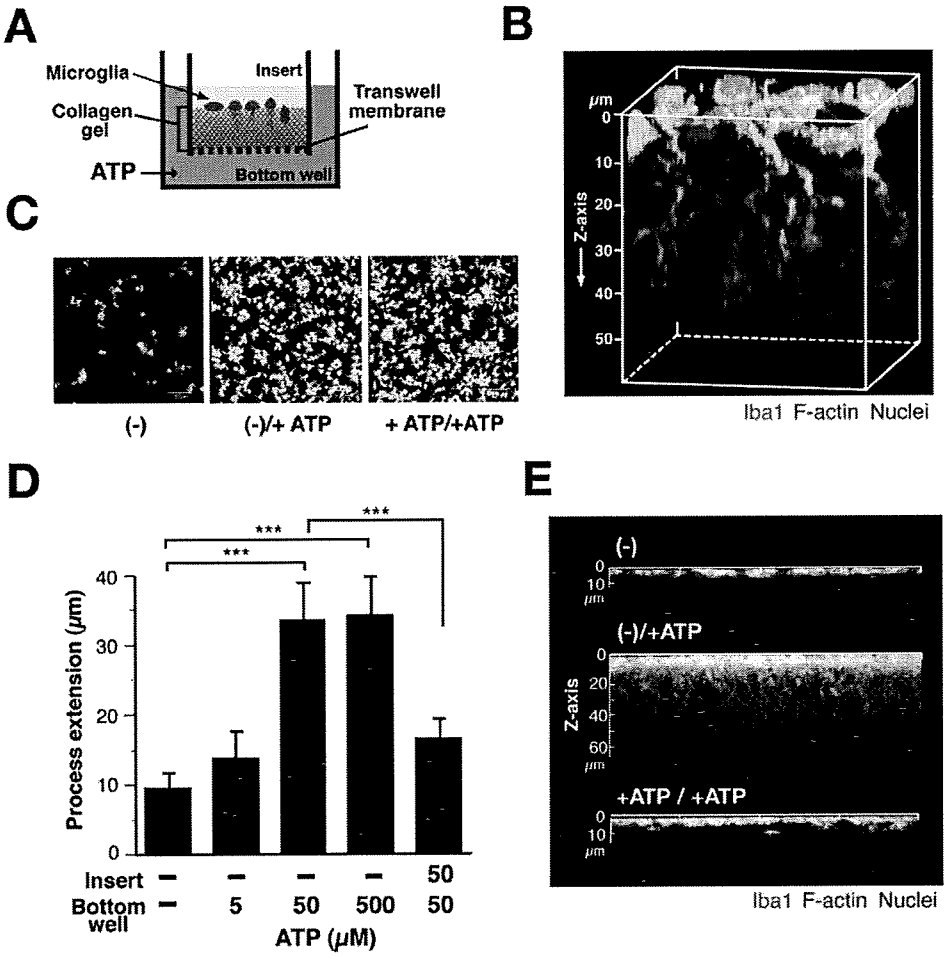

Fig. 1. ATP induces chemotactic process extension by microglia in 3D collagen gels. (**A**) Schematic diagram of the assay system for microglial process extension. Rat primary-culture microglia are plated on collagen gels in the insert well of a transwell chamber and stimulated by ATP addition to the bottom well. (**B**) At 2 h after ATP addition to the bottom well, microglia were fixed and stained with DAPI (blue), anti-Iba1 antibody (green), and phalloidin (red). A 3D image of microglia is reconstructed from XY-images acquired at 2 μm z-step intervals through a confocal microscope. The surface of the gels is located at zero on the *Z*-axis. Microglia extend processes into the gels toward ATP. (**C**) Microglia remaining in the gels 2 h after the addition of DMEM (–) or 50 μM ATP (–/+ATP) to the bottom well, or simultaneous addition of 50 μM ATP to both the insert well and the bottom well (+ATP/+ATP). Maximum projection of Iba1-positive signals is reconstructed by stacking XY-images in the direction of the *Z*-axis. Scale bar, 50 μm. (**D**) Quantification of microglial process extension 2 h after addition of ATP to the bottom well, or simultaneous addition of ATP to both the insert well and the bottom well. ***$P < 0.001$, $n = 3$–4 for each set of conditions; Student's *t*-test; mean ± S.D. (**E**) Representative images of microglia after stimulation for 2 h. Maximum projection of each signal is constructed by stacking in the direction of *Y*-axis. The surface of the gels is located at zero on the *Z*-axis.

integrin-β subtypes on process extension. The results showed that a functional blocking antibody against integrin-β1 (20 μg/mL) significantly inhibited process extension, but that the antibody against integrin-β3 (20 μg/mL) did not (Fig. 3B). These results indicate that integrin-β1 is involved in process extension by microglia.

ATP/ADP Promote Microglial Adhesion to Collagen Gel Through Integrin-β1

We next performed a cell adhesion assay to determine whether ATP increases microglial adhesion to collagen gels through integrin-β1. Following stimulation with ATP, the microglia were plated on gels and incubated for 1 h, and the cells that had attached to the gels were counted. ATP (50 μM) increased microglial adhesion to the gels, and ADP (50 μM) increased microglial adhesion the same as ATP (Fig. 4A). AR-C69931MX completely suppressed the ATP/ADP-induced increase in cell adhesion, indicating that $P2Y_{12}$ mediates the increase. To determine whether integrin-β1 is involved in the ATP/ADP-induced increase in microglial adhesion to the gel, we examined the effect of RGD peptides and a functional blocking antibody against integrin-β1 on cell adhesion. After pretreating microglia with 30 μM RGD peptides, the cells were stimulated with ATP/ADP and plated on gels. The RGD peptides significantly inhibited the ATP/ADP-induced increase in cell adhesion, but the RGE peptides (30 μM) did not (Fig. 4B). Pretreatment of microglia with a functional blocking antibody against integrin-β1 (5 μg/mL) significantly suppressed the increases in the

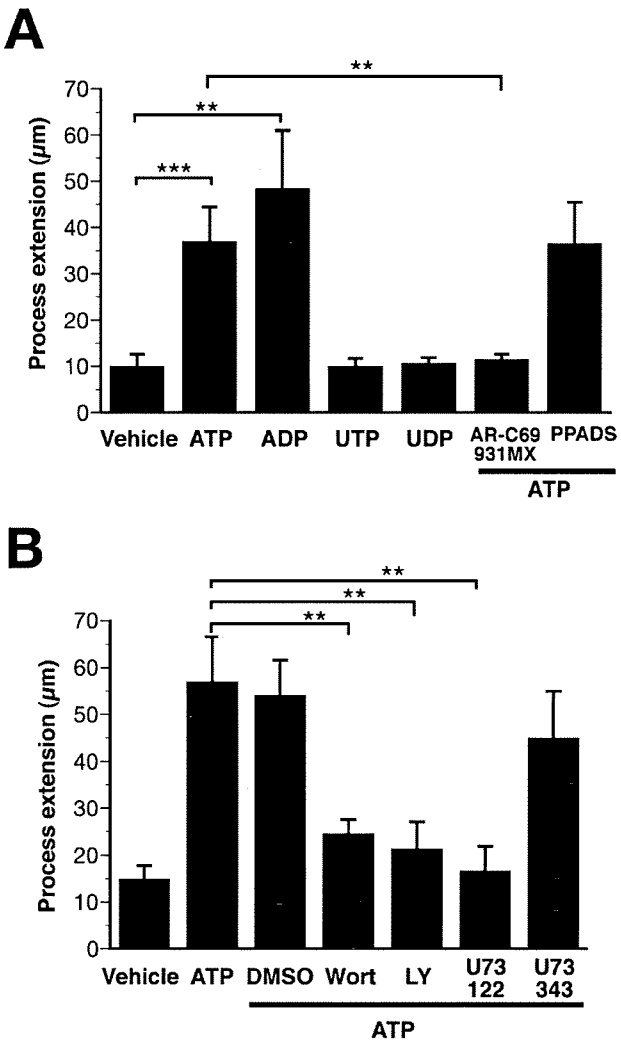

Fig. 2. ATP-induced process extension by microglia requires activation of PI3K and PLC signaling pathways downstream of $P2Y_{12}$. (**A**) Quantification of microglial process extension 2 h after stimulation with DMEM (vehicle), ATP (50 μM), ADP (50 μM), UTP (500 μM), or UDP (500 μM), and stimulation with ATP (50 μM) following pretreatment with AR-C69931MX (1 μM) for 10 min or PPADS (100 μM) for 10 min. (**B**) Effect of PI3K and PLC inhibitors on ATP-induced process extension. Microglia were stimulated with ATP (50 μM) for 2 h after pretreatment with DMSO (0.04%), Wortmannin (2 μM), or LY29004 (50 μM) for 10 min, or with U733122 (100 nM) or U73343 (100 nM) for 5 min. ***$P < 0.001$; **$P < 0.01$; n = 3–4 for each subsance; Student's t-test; mean ± SD.

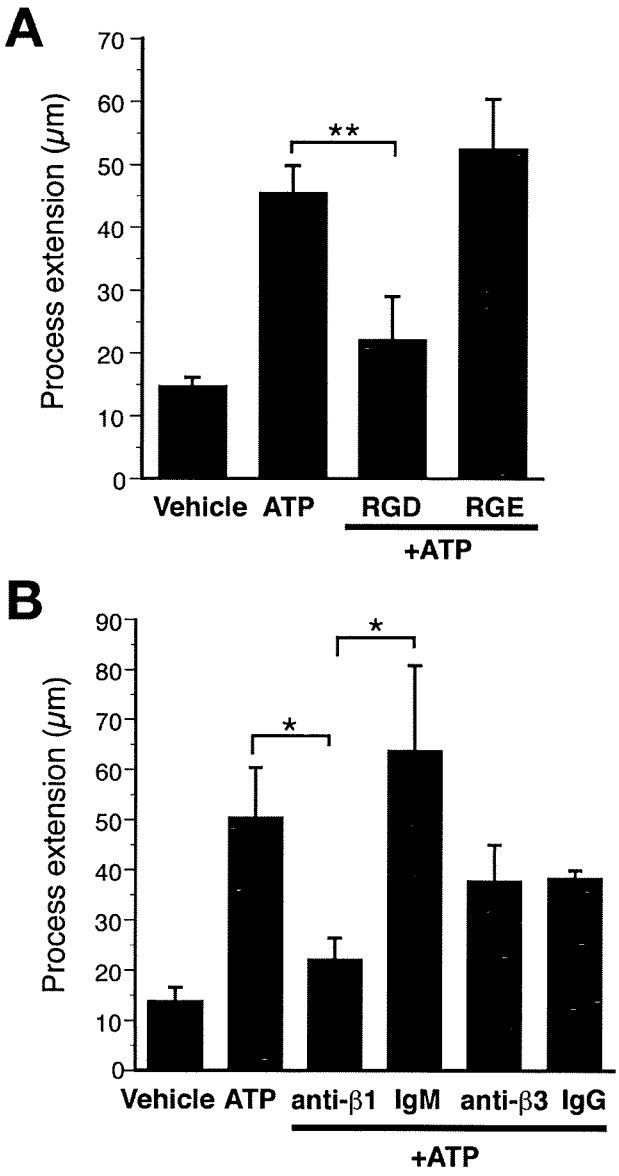

Fig. 3. RGD peptides and a functional blocking antibody against integrin-β1 inhibit ATP-induced process extension. (**A**) Quantification of microglial process extension at 2 h after stimulation with DMEM (vehicle) or ATP (50 μM) following pretreatment with RGD peptides (300 μM) or RGE peptides (300 μM) for 30 min. (**B**) Microglia were pretreated for 1 h with 20 μg/mL of functional blocking monoclonal antibody against integrin-β1 or integrin-β3, or isotype control monoclonal antibodies, and then stimulated with ATP (50 μM) for 2 h. Control hamster IgM and IgG were used as the control for anti-integrin-β1 antibody and anti-integrin-β3 antibody, respectively **$P < 0.01$, *$P < 0.02$; n = 3–4 for each substance; Student's t-test; mean ± SD.

cell adhesion (Fig. 4C), but pretreatment with normal hamster IgM (5 μg/mL) instead of the anti-integrin-β1 antibody had no inhibitory effect. These results indicate that integrin-β1 participates in ATP/ADP-induced increase in microglial adhesion to gels and suggest that ATP/ADP induces activation of integrin-β1.

ATP-Stimulated $P2Y_{12}$ Mediates Integrin-β1 Activation

To determine whether ATP activates integrin-β1 through $P2Y_{12}$, we measured integrin-β1 activation by ATP in 1321N1 cells that stably expressed HA-tagged rat $P2Y_{12}$ (1321N1-P2Y12). The results showed that the level of total integrin-β1 protein expression in 1321N1-P2Y12 cells was the same as in wild-type 1321N1 cells (Fig. 5A). The level of activated integrin-β1 in the cell lysates was measured by immunoprecipitation with an antibody against the active form of integrin-β1. When 1321N1-P2Y12 cells were stimulated with ATP, the active integrin-β1 level had increased significantly at

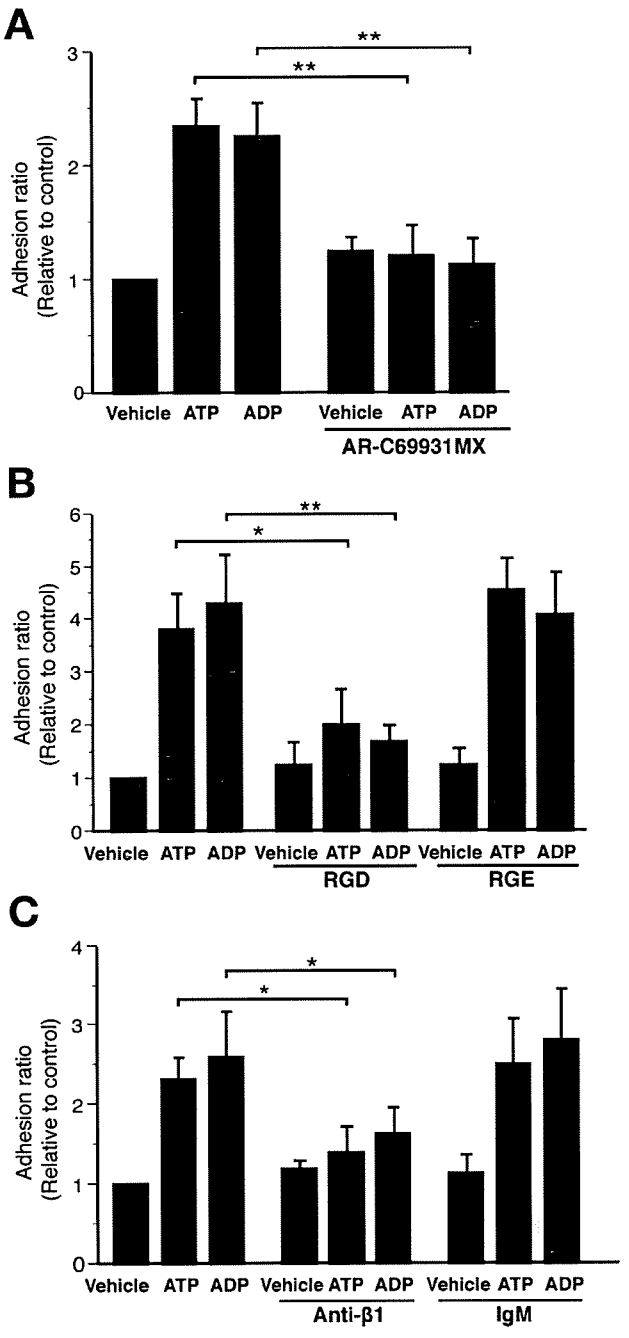

Fig. 4. ATP increases microglal adhesion to collagen gels through integrin-β1. (**A**) Microglia preincubated for 10 min in the presence or absence of AR-C69931MX (1 μM) were stimulated with DMEM (vehicle), ATP (50 μM) or ADP (50 μM) and plated onto the gels. After incubation for 1 h, cells that had attached to the gels were counted. Cell adhesion is expressed as the ratio of the number of stimulated cells that had attached to the number of cells that had attached under control conditions. (**B**) Microglia preincubated with RGD (30 μM) or RGE (30 μM) peptides for 10 min were stimulated with ATP (50 μM) or ADP (50 μM). (**C**) Microglia preincubated with 5 μg/mL of anti-integrin-β1 antibody or control hamster IgM for 10 min were stimulated with ATP (50 μM) or ADP (50 μM). $^{**}P < 0.01$, $^{*}P < 0.05$; $n = 3$–4 for each substance; Student's t-test; mean ± SEM.

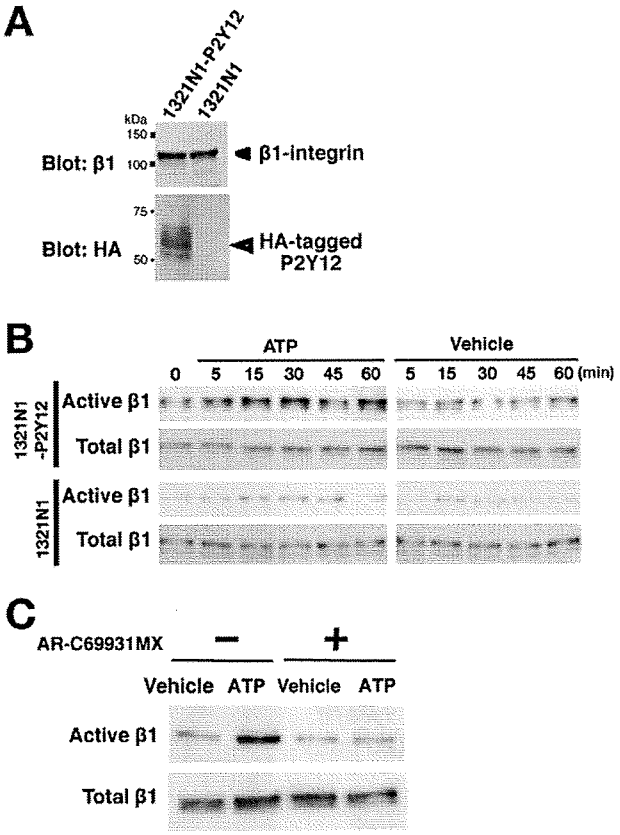

Fig. 5. ATP induces activation of integrin-β1 through $P2Y_{12}$. (**A**) 1321N1 cells stably expressing rat HA-tagged $P2Y_{12}$ (1321N1-P2Y12) and wild 1321N1 cells were analyzed for expression of integrin-β1 and HA-tagged $P2Y_{12}$ by Western blot analysis with anti-integrin-β1 antibody (clone 18) and anti-HA antibody (clone 3F10, Roche), respectively. (**B**) 1321N1-P2Y12 cells and 1321N1 cells were stimulated with vehicle (DMEM) or 100 μM ATP for the periods of time indicated and lysed in lysis buffer. The active form of integrin-β1 (active β1) in each cell lysate was immunoprecipitated with an antibody against active integrin-β1 (HUTS-4). Integrin-β1 in the cell lysates and the immunoprecipitated samples was detected by Western blot analysis with anti-integrin-β1 antibody (clone 18). (**C**) 1321N1-P2Y12 cells were pre-incubated in the presence or absence of AR-C69931MX (2 μM) for 10 min and stimulated with DMEM (vehicle) or ATP (100 μM) for 30 min. Similar results were obtained in three independent experiments.

5 min, and the activation was sustained for 1 h (Fig. 5B), whereas the level of active integrin-β1 in wild-type cells was not significantly increased by ATP stimulation. Stimulation with medium alone had no effect on the level of active integrin-β1 in 1321N1-P2Y12 cells or wild-type cells. Preincubation with AR-C69931MX (1 μM) completely prevented the integrin-β1 activation induced by ATP in 1321N1-P2Y12 cells (Fig. 5C). These results clearly indicate that $P2Y_{12}$ mediates the activation of integrin-β1 following ATP stimulation.

Integrin-β1 Expression by Ramified Microglia in Normal Brain

Previous studies have shown that primary-culture microglia express integrin-β1 (Kloss et al., 1999; Nasu-Tada et al., 2005), and immunostaining with the

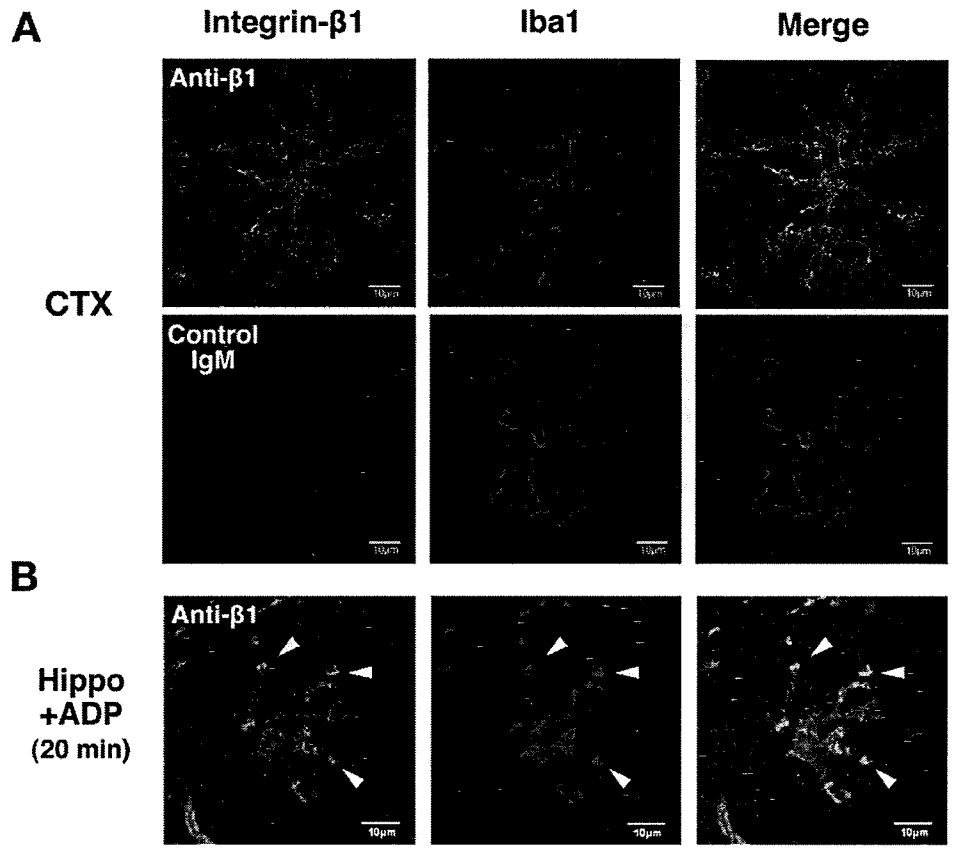

Fig. 6. Integrin-β1 is expressed in microglia in brain tissue. (**A**) Microglia in cortical slices from adult rats were examined for integrin-β1 immunoreactivity. Punctate integrin-β1 (green) signals are observed in Iba1-positive cells (red). There are no control hamster IgM signals in the microglia. Scale bar, 10 μm. (**B**) Rat neonatal hippocampal slices incubated for 1 h in oxygenated culture medium were transferred onto a chamber, and 1 mM ADP was added to the bath medium as described in Materials and Methods. After 20 min the slices were fixed and stained with anti-integrin-β1 antibody (green) and anti-Iba1 antibody (red). The photographs show a microglial cell in the stratum pyramidale of the CA3 area of the hippocampus. The periphery of the slice in each frame is at the right. The microglia extend their processes toward the periphery of the slices. Arrowheads indicate the tips of the microglial projection where integrin-β1 has accumulated. Scale bar, 10 μm.

antibody against integrin-β1 (clone Ha2/5) in this study showed that integrin-β1 was in fact expressed in rat primary-culture microglia and that it was localized in their processes after ATP stimulation (data not shown). To determine whether integrin-β1 is expressed by microglia in rat brain parenchyma, sections of cerebral cortex were immunohistochemically stained with the anti-integrin-β1 antibody (clone Ha2/5) and anti-Iba1 antibody. As shown in Fig. 6A, integrin-β1-immunopositive signals were observed in Iba1-immunoreactive cells, which are ramified microglia that have a small cell body and highly branched processes. The punctate integrin-β1 signals were localized along the microglial processes. Thus, our findings showed that integrin-β1 is expressed by ramified microglia.

Integrin-β1 Accumulation in the Tips of Microglial Processes Extending Toward a Nucleotide Source in Brain Tissues

Recent imaging studies have shown that following the addition of ADP to the culture medium microglia in rat and mice hippocampal slices extend their processes and migrate toward the periphery of the slices, and the studies have demonstrated that these phenomena are mediated by $P2Y_{12}$ (Haynes et al., 2006; Kurpius et al., 2007). To examine the intracellular localization of integrin-β1 in microglia that had extended processes in brain tissue after ADP stimulation, hippocampal slices prepared from neonatal (p4-8) rats were exposed to 1 mM ADP for 20 min, and then fixed and stained with the integrin-β1 antibody and anti-Iba1 antibody. As shown in Fig. 6B, Iba1-positive cells extended processes toward the periphery of the slices, and integrin-β1-positive signals appeared to be localized at the tips of the processes of Iba1-positive microglia.

RGD Peptides Inhibit ADP-Induced Process Extension by Microglia in Hippocampal Slices

To determine whether integrin-ECM interaction is required for $P2Y_{12}$-dependent process extension by microglia in brain tissue, we examined the effect of the RGD peptides on the process extension by microglia in

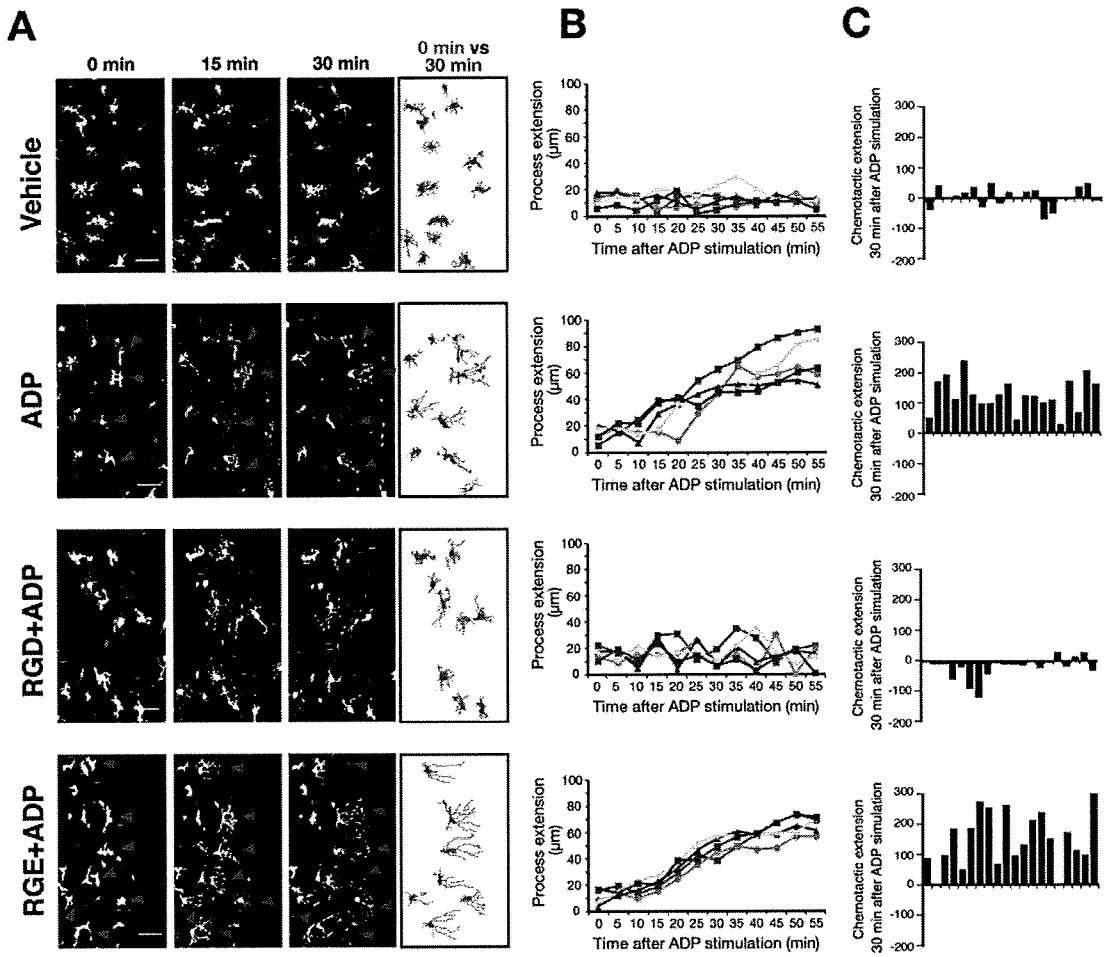

Fig. 7. RGD peptides inhibit the process extension by microglia responding to exogenous nucleotides in brain slices. (**A**) Microglia in hippocampal slices from neonatal (p4-7) EGFP-expressing mice were examined by time-lapse confocal imagng. Microglia extended long processes (red arrowheads) toward the periphery of the slices (right side of each frame) at various time points following addition of 1 mM ADP to the bath. In the presence of 1 mM RGE peptides microglia extended processes toward the periphery of the slices, whereas no long process extension toward the periphery of the slices was observed in the presence of 1 mM RGD peptides. Morphology of microglia at time 0 (green) and 30 min later (red) is depicted in the panel on the far right. (**B**) Microglial process length (μm) in slices measured at each time point indicated (five processes per cell). Positive length change indicates extension, whereas negative length change indicates retraction. RGE-treated microglia continuously extended their processes, whereas RGD-treated microglia repeatedly extended and retracted their processes. (**C**) Chemotaxis of the process extension responding to ADP addition in the absence and presence of RGD and RGE peptides. The degree of chemotactic extension (μm) of each cell is expressed by the difference obtained by subtracting the total length of the branches extending away from the nucleotide source from the total length of branches extending toward the periphery of the slices. Twenty cells residing in the stratum pyramidale and stratum oriens of the CA3 area of the hippocampus were examined 30 min after the addition of ADP. In the presence of RGE peptides, microglia extended their processes toward the ADP source the same as when stimulated with ADP alone, whereas directional process extension decreased in the presence of RGD peptides.

hippocampal slices prepared from neonatal (p4-7) Iba1-EGFP transgenic mice (Hirasawa et al., 2005), whose microglia are easily detected by EGFP signals. To analyze the initial response of microglia to ADP, we monitored the behavior of microglia expressing EGFP by time-lapse microphotography for 1 h following exposure to 1 mM ADP in the bath. The microglia in unstimulated slices repeatedly extended and retracted processes a short distance, but their cell bodies did not migrate. When slices were exposed to ADP, most of the microglia did not migrate from their original position for a period of 1 h and they rapidly extended their long processes toward the periphery of the slices within 5 min, and the extension was sustained for 1 h (Fig. 7A, Supp. Info. Video 1). We confirmed that the process extension in the ADP-stimulated slices was suppressed by treating the slices with AR-C69931MX (10 μM), indicating that $P2Y_{12}$ mediated the process extension by microglia in the culture slices (data not shown). Pretreating slices with RGD peptides (1 mM) significantly inhibited the rapid process extension by microglia toward the periphery of the slices, whereas pretreating slices with RGE peptides (1 mM) had no effect on the process extension by microglia (Fig. 7C,D, Supp. Info. Video 2). Following ADP exposure, the microglia in the RGD-pretreated slices sent out many processes in random directions, and

the processes were often extended to nearly 40 μm but immediately retracted. These findings indicate that blocking of the integrin-ECM interaction with RGD peptides suppressed directional process extension by microglia in brain tissue.

DISCUSSION

In this study, we used collagen gel to establish an *in vitro* assay system to analyze the molecular mechanisms that regulate process extension by microglia. Morphological changes and migration by microglia have previously been studied by using two-dimensional culture systems, such as the Boyden chamber (Nolte et al., 1997) or the Dunn chemotaxis chamber (Honda et al., 2001; Webb et al., 1996). However, it has not been possible to reproduce the directional process extension by microglia observed in brain tissues with these systems. The cell culture system using 3D matrices is known as a model that mimics the state of cells in tissue and has been reported to be useful for examination of cell motility and signaling events (Cukierman et al., 2002). We therefore plated microglia on 3D-collagen gels in the insert of a transwell chamber, and we were able to show that the cells extended their processes into the gels in an ATP-gradient-dependent manner.

Our findings strongly suggest that an integrin-β1-ECM interaction is involved in the directional process extension. Microglial adhesion to collagen gel was weak under unstimulated conditions, and ATP increased the strength of the microglial adhesion to the gel. The RGD peptides and the functional blocking antibody against integrin-β1 inhibited the cell adhesion and the process extension into the gels, and the RGD peptides significantly inhibited ADP-induced process extension by microglia in hippocampal slices. ECM molecules that bind to integrin-β1, such as fibronectin, vitronectin, and laminin, have been reported to be slightly expressed in the normal brain and localize in microblood vessels (Bellail et al., 2004; Krum et al., 1991). Previous studies have shown that microglia attach weakly to laminin and ECM of astrocytes, and that laminin exerts a dominant anti-adhesive effect on microglial adhesion to astrocytes (Milner and Campbell, 2002b). Accordingly, most of the integrin-β1 in microglia in the normal brain seems to be inactivated. Collagen type-I is considered to be an artificial substrate for microglia because neither collagen fibers nor collagen-rich basal laminas are present in the CNS (Jones, 1996). However, the weak adhesion by microglia to collagen gels suggest that the microglia cultured in the gels maintain integrin-β1 in an inactivated state, the same as microglia in brain tissue. Accumulating studies have demonstrated that laminins are expressed by astrocytes and neurons in the adult brain and are involved in axon growth and guidance (Grimpe et al., 2002; Jucker et al., 1991; Liesi, 1990; Zhou, 1990). We confirmed that microglia attach weakly to laminin-coated dishes and that ATP induces an increase in microglial adhesion to laminin (data not shown). These observations suggest that laminins are candidates for the molecules that bind integrin-β1 to achieve the ATP/ADP-induced process extension by microglia in brain tissue.

In the normal brain, microglia express integrin-β2, LFA1 (αLβ2), and CD11b/CD18 (αMβ2) (Kloss et al., 1999). Previous studies have shown that the rapid change in microglial morphology and migration by microglia toward injured neurons in hippocampal slices are unaffected in tissue slices from integrin-β2 deficient mice (Kurpius et al., 2006). Although these studies suggest that integrin-β2 is not involved in the early activation of microglial motility, we were unable to completely rule out a role of integrin-β2 in process extension. Further study will be necessary to identify the subtypes of integrins that are involved in the rapid process extension in brain tissue.

The increase in cell adhesion requires that integrins become "activated" by undergoing conformational changes regulated by inside-out signals (Hynes, 2002; Kinashi, 2005). ATP/ADP increased the microglial adhesion to collagen gels, and the increase was inhibited by RGD peptides, a functional blocking antibody against integrin-β1, and a $P2Y_{12}$ selective antagonist, AR-C69931MX. ATP increased the active integrin-β1 level in $P2Y_{12}$-expressing 1321N1 cells but not in wild-type cells. These results demonstrate that $P2Y_{12}$ mediates the ATP-induced activation of integrin-β1. Stimulation of G protein-coupled receptors activates several signaling pathways, including the PI3K, PLC, RAS, and Rho family small GTPase, and mitogen-activated protein kinase (MAPK) signaling cascades, some of which have been implicated in the inside-out signaling (Hynes, 2002; Kinashi, 2005). In this study, we showed that activation of both PI3K and PLC signaling pathways downstream of $P2Y_{12}$ is required for the ATP-induced process extension by microglia. In addition, we examined the effect of PI3K and PLC inhibitors on the ATP-induced increase in microglial adhesion to collagen gels. Pretreatment with the PLC inhibitor U73122 (100 nM) inhibited cell adhesion, whereas the PI3K inhibitor LY294002 (50 μM) had no effect (data not shown), suggesting that PLC activation is required for activation of integrin-β1 but that PI3K activation is not. Previous studies have demonstrated that binding of the cytoplasmic actin-bindng protein talin to the β integrins tail is crucial for the activation of β integrins (Tadokoro et al., 2003), and the small GTPase Rap1 has been reported to regulate talin binding to β integrins through C-kinase and calcium signaling pathways downstream of PLC (Franke et al., 1997, 2000; Han et al., 2006). Thus, Rap1-Talin cascades may be involved in $P2Y_{12}$-mediated activation of integrin-β1 in microglia. However, further works are needed to determine which of the aforementioned regulatory mechanisms is relevant in microglia.

As described in previous reports (Haynes et al., 2006; Kurpius et al., 2007), time-lapse imaging of EGFP-labeled microglia in hippocampal slices showed that addition of ADP to the bath immediately induced process extension by microglia toward periphery of the slices.